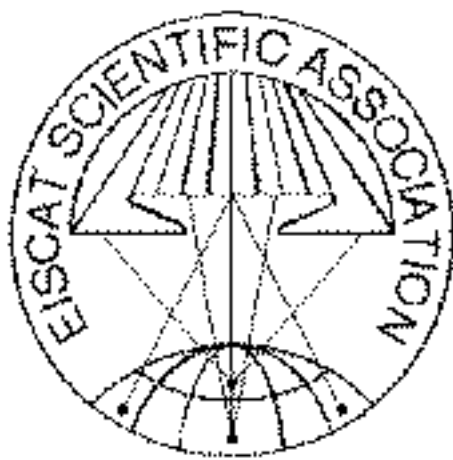


REPORT ON UK EISCAT RESEARCH IN 1998 AND 1999

Prepared on behalf of the UK EISCAT Community by

Dr. I.W. McCrea and Miss L. Williams

Rutherford Appleton Laboratory



Cover Illustration: The EISCAT Svalbard Radar, as seen from the mountain behind the site in August 1999, just after the completion of the second dish. (*Photograph courtesy of Ingemar Wolf*).

Index

1.	Foreword	page	3
2.	Introduction		4
3.	Development of the EISCAT radars during 1998 and 1999		4
4.	Mesosphere and D-region		6
5.	Auroral Studies		8
6.	Instabilities		16
7.	Electrodynamics		17
8.	Ionosphere-Thermosphere Interactions		17
9.	Large-Scale Structures		19
10.	Artificial Heating		24
11.	ULF Waves		27
12.	EISCAT/CUTLASS Studies		30
13.	Magnetosphere-Ionosphere Coupling and Reconnection		32
14.	The Solar Wind		37
15.	Instrumentation and Techniques		40
	Appendix A: Papers produced by the UK EISCAT community		41
	Appendix B: UK EISCAT campaigns in 1998 and 1999		47
	Appendix C: The UK EISCAT user community		55

1. Foreword

This report summarises the scientific highlights of the research programmes undertaken by the UK EISCAT community during 1998 and 1999. In addition, it includes appendices providing details of the scientific papers including EISCAT results published during 1998 and 1999, the EISCAT campaigns organised in those two years, and a list of the names and contact addresses of the entire UK EISCAT community. The report is intended to provide input to EISCAT's own two-yearly international report to be published in summer 2000.

These last two years have been extremely important in the development of the EISCAT Scientific Association, as well as being a very active period of EISCAT-related research. On the technical side, the rapid development of the EISCAT Svalbard Radar, with new modes to allow clutter-free E-region observations, and the construction and successful operation of the new fixed dish were major highlights. An extensive programme of upgrades and refurbishments to the mainland radars is underway at the time of writing, which will result in many improvements in the capabilities of the UHF and VHF systems. The research results reported here include innovative studies by UK scientists over the whole range of Solar-Terrestrial Physics. They range from new measurements of the solar wind as it evolves towards solar maximum, through the first use of the ESR for the studies of dayside coupling with the magnetosphere, to unprecedentedly high-resolution observation and modelling of the aurora.

One of the most important roles played by EISCAT over the period covered by this report has been to make key measurements in conjunction with other facilities. The joint operation of the EISCAT radars and the Heater has enabled artificially generated ULF waves to be produced for the first time, opening up the exciting possibilities of field-line tagging. The use of optical facilities with the Tromsø radars and the heater has produced the first definitive observations of stimulated airglow ever measured at such high latitudes. The use of optical systems in conjunction with the ESR is providing new insight into coupling processes and has proved invaluable for placing the radar results in context. The combined use of EISCAT and CUTLASS has improved the understanding of F-region irregularities and produced unexpected opportunities in the study of ULF waves.

The next two years look set to be an even more significant period, with the re-launch of the CLUSTER satellites scheduled for June and July of this year, and the likelihood that the new experimental modes available after the refurbishment of the mainland radars will extend their coverage and accuracy. The range of activities documented in this report bears witness to the continuing vigour and diversity of the UK EISCAT community and demonstrates that it should be in an excellent position to exploit these opportunities to the full.

Ian McCrea and Liz Williams

March 2000

2. Introduction

The structure of this report is similar to that published in 1998. As before, the section headings reflect the different research priorities evident over the last two years. Research themes whose development was beginning at the time of the previous report have come increasingly to the fore. In particular these changes in research priorities reflect an increased emphasis on high-latitude coupling, generation and study of ULF waves and the use of EISCAT in conjunction with other STP facilities.

During the two years covered by this report, 52 papers by members of the UK EISCAT community have been published in refereed journals. The 1999 EISCAT International Workshop was held in Wernigerode, Germany and the UK provided the largest national contingent attending the meeting, with UK authors contributing to 30 papers. Many of these are currently going through the review process – at least 30 UK EISCAT papers are awaiting publication. A further 4 PhD theses have been awarded in the UK for research work involving the EISCAT radars, demonstrating that EISCAT data continue to serve as a training ground for the development of new UK scientists.

The UK community has continued to be very active in experimental work on the EISCAT radars over the period of this report. The UK allocation of mainland EISCAT time was used right up to the available capacity and the use of the Svalbard radar, although not yet at the same level, is increasing. An increasing number of campaigns have been organised in collaboration with other EISCAT countries, with data being pooled among the participants. This has meant that although 610 hours of accounting time were used in running UK experiments during 1998 and 1999, 1367 hours of Special Programme data have actually been returned to the UK. Twelve campaigns were carried out during the last two years, during which 24 different UK experiments were run on behalf of principal investigators from seven institutions. UK scientists once again collaborated with colleagues in every other country of the EISCAT Scientific Association, and several outside it. Experiments have included one of the longest-ever continuous runs in the history of incoherent scatter, for the study of tides and their modulation by planetary waves, and the first UK Special Programmes on the fixed dish of the EISCAT Svalbard Radar. Twenty-eight UK scientists participated in campaign operations, of which 10 were trainees. These figures are the same as in the previous two years, and show the continuing interest among new research students and RAs in running experiments at the EISCAT radars.

3. Development of the EISCAT Radars during 1998 and 1999

The most significant developments during 1998 and 1999 occurred at the EISCAT Svalbard Radar (ESR). The two most important of these were the implementation of an experimental mode which totally removed the clutter contribution from the data, allowing routine observations down to 90 km, and the construction and acceptance of the second dish. The clutter reduction has been accomplished by an elegant technique using pulse-to-pulse subtraction. The principle is that two identical pulse groups are used, whose separations are longer than the correlation time of the plasma waves being studied, but shorter than the correlation time of the contaminating clutter. Subtracting the two sample sets removes the clutter while leaving the target and noise contributions, which are independent in each pulse. The only overhead is that the integration and stationarity times are doubled by the need to transmit the modulation twice, but the benefits of the clutter reduction far outweigh this disadvantage. The technique was first tested in March 1998, and since August 1998 it has been in regular use in a radar programme known as gup3, which combines alternating code and long pulse measurements to deliver profiles of plasma parameters for all altitudes from 90 to 1000 km.

The contract for the provision of the second ESR dish was signed with Alcatel Telespace (France) in February 1998. Work on preparing the foundations for the dish began in August 1998, and the first experiment using the new antenna was run on 8th and 9th October 1999. The new dish is a 42m rotationally symmetric Cassegrain design, with 45.3 dBi gain and low sidelobes. It is fixed in the field-aligned direction, although steerability of about 1° can be achieved by offsetting the feed (but this is a long process). The second dish will make all field-aligned measurements at the ESR from now on, and the steerable dish will be prevented from looking in the field-aligned direction in order to prevent unwanted interferometric effects. Pulse-to-pulse switching of the transmitter power between the two antennas should ultimately be possible, though technical difficulties have prevented this so far. During 1998, the power of the ESR transmitter was increased from 0.5 MW to 1 MW with the addition of

eight new klystron modules. A new lubrication system was installed following problems with the control system of the steerable antenna. Plasma line channels have also been installed at the ESR, but are currently being used for tests of the new antenna. The EISCAT Svalbard Radar got its first permanent staff in 1998, and in that year the ESR was the most heavily used of all the EISCAT facilities, running 1031 hours. A ten-day experiment in July 1999 (also run by the mainland UHF system) was one of the longest continuous experiments in the history of incoherent scatter radars.

On the mainland, serious transmitter problems were experienced after October 1998 when EISCAT's last fully-working UHF klystron failed. The spare klystron was not capable of transmitting all of the modulation schemes currently used in EISCAT experiments, although the situation has improved considerably as the klystron has aged. A plan was made to replace the UHF klystron with new modules built by Thomson CSF (France). These new klystrons, which will be installed in the first half of this year, will raise the transmitted power limit at Tromsø to 2.5 MW. In addition, a new receiver front end has been installed at the Tromsø site (purchased as an in-kind contribution from Germany and UK) which has reduced the system noise temperature of the UHF system from 110K to 78K. The new klystron and front end together should be capable of making an order of magnitude improvement in measurement accuracy at Tromsø, and the new klystrons should also deliver a factor of 2 improvement at the remote sites.

Plans have also been made to refurbish the receiver chain and computing system of the mainland radars, and this work is underway at the time of writing. The old (mostly analogue) receiver systems will be replaced with new technology in which the signal processing is done digitally. The mainland system will not use the same Digital Signal Processors (DSP) used in the construction of the ESR, since the performance of these can be bettered by modern commercially available computer chips. The DSPs at the ESR will eventually also be replaced by commercial technology. Several failures of the ND computers at the mainland sites have meant that these machines will be replaced by modern Unix-based systems, meaning that the old control languages for EISCAT (EROS, ELAN and TLAN) will also be replaced. The speed of the internet connections to the Tromsø site has also been upgraded.

The heating facility has been used more heavily than for several years, and its use has yielded some of the most interesting results obtained by EISCAT during the period of this report. A new operating agreement has extended the number of available frequencies and the computer control of the heater has been upgraded. The Dynasonde has also been upgraded and a new control computer installed. A number of new sounding schemes have added to the range of measurements that the instrument can perform.

Jürgen Röttger left the post of EISCAT Director in January 1998 after 11 years and was replaced by Tauno Turunen. The main data archive was moved from Kiruna to Tromsø, and responsibility for staff employment at Sodankylä was passed from the Finnish Academy to the University of Oulu. A successful EISCAT International Workshop was held in Wernigerode, Germany in October 1999, and the next workshop has been scheduled for Japan in 2001.

The following sections summarise the highlights of research work carried out using the EISCAT facilities by UK scientists during 1998 and 1999.

4. Mesosphere and D-Region

The Mesosphere/Lower-Thermosphere Neutral Dynamics Group at the University of Wales Aberystwyth have investigated the coupling and dynamics of this poorly understood region of the atmosphere. The studies have involved using the database of EISCAT CP-6 vertical velocities to reveal gravity waves at mesopause heights. The results of this study suggest the vertical velocity motion field is dominated by gravity waves, and that frequently these waves are ducted (Mitchell & Howells, 1998). The initial studies prompted further work to elucidate the nature of the ducting processes. Such studies are particularly important because gravity waves are known to play the key role in the transport of energy and momentum from the lower atmosphere to mesospheric and thermospheric heights, where momentum deposition has a profound influence on the general circulation of the atmosphere. A full understanding of the phenomena controlling the gravity-wave field at these heights is therefore vital in understanding the planetary-scale atmospheric circulation.

An example of a possible ducted gravity wave is presented in figure 1, which presents vertical velocity data recorded by the CP-6 experiment of 31 July 1992. A strong periodic motion is evident at heights of 78-86 km between 06:00-12:00 UT, and this is attributed to a gravity wave with a period of about 30 minutes. The vertical velocities arising from this motion diminish almost to zero at the upper and lower boundaries. This amplitude profile may result from large vertical shears in the horizontal wind creating regions above and below in which the gravity wave cannot propagate. In effect, the horizontal wind creates a horizontal wave-guide in which the gravity wave propagates. To further investigate this process, simultaneous observations of vertical and horizontal velocities are necessary to reveal both the wave and the proposed duct.

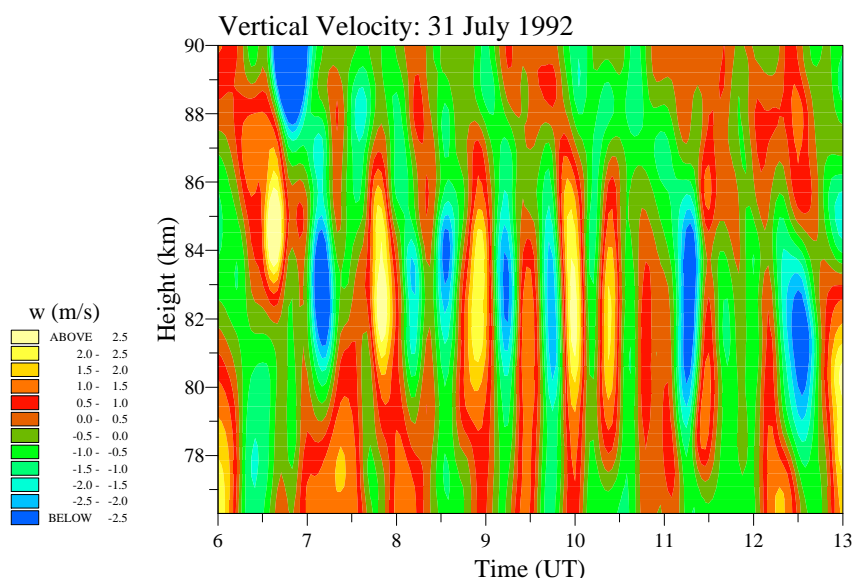


Figure 1 Time-height contour plot of vertical velocity derived from EISCAT-VHF CP-6 observations on 31 July 1992.

The EISCAT special program SP-UK-DUCT experiment is identical to the CP-6 experiment except that the EISCAT VHF antenna is used in a split-beam mode, with one half of the antenna pointing vertically and the other half pointing off-vertically by about 15° . From the radial velocities measured by the off-vertical beam, horizontal velocities are inferred so that simultaneous measurements of horizontal and vertical velocities can be made. SP-UK-DUCT has been run on two occasions. A short 8-hour experiment was performed in March 1998 to test the feasibility of the experiment and a second, longer run of 30 hours was performed in May 1999. Vertical and horizontal velocities measured during the test run of the DUCT experiment are presented in figure 2 as time-height contour plots of vertical and horizontal winds. The wind field was very quiet during this observation period and unfortunately no obviously ducted waves were observed. During the second experiment, the antenna beam was phased off-vertically which reduced the collecting volume of the radar beam significantly. In hindsight, the experiment would not have been run in this configuration because there was not enough backscattered signal to make any useful observations. The success of the first test run has demonstrated that this experiment works well and should be re-run in the future.

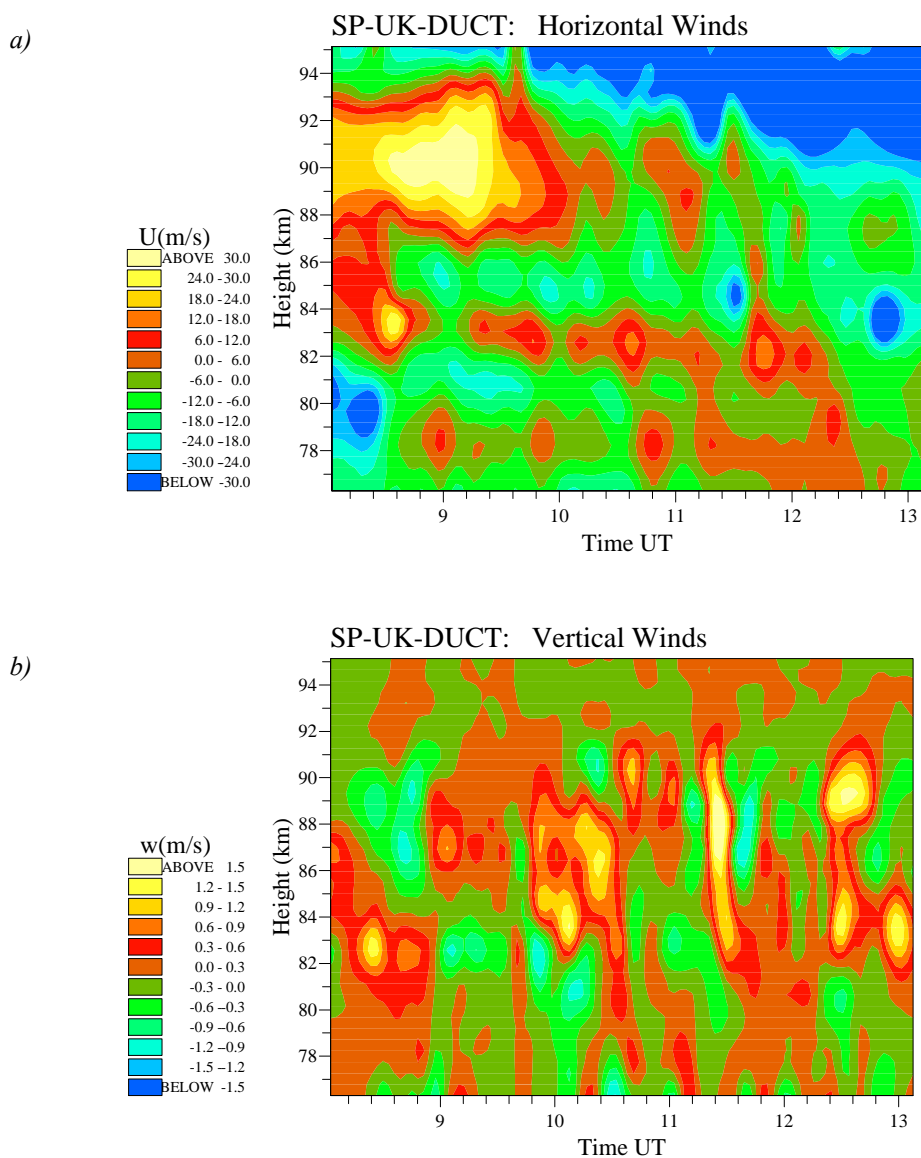


Figure 2 Time-height contours of horizontal velocity (a) and vertical velocity (b) measured during the test run of SP-UK-DUCT (30 March 1998).

An international PMSE (Polar Mesosphere Summer Echoes) campaign in June 1998 resulted in some interesting VHF data that seems to confirm roughly the predictions of work at University College London by Yvan Chaxel. His theory of the dependency of PMSE on ice particle size gives a way of estimating the ice particles' radii from the radar return. Although the 1998 date was not as good as had been hoped, analyses of the best of it suggests the ice particle sizes deduced were roughly what would be expected from modelling studies.

5. Auroral Studies

Research at the University of Southampton has concentrated on the development of modelling work which links the source region of field-aligned currents in the inner magnetosphere with the effects measured in the auroral ionosphere. Recent results have shown that ohmic heating in the ionosphere can act as evidence for the presence of field-aligned currents. The work combines observations from EISCAT with high spatial and temporal resolution optical images. Observations have been made on several occasions of sudden increases in electron temperature, which occur immediately before an arc enters the radar beam and in a clear minimum of electron density. This can be seen in the middle panel of figure 3, which shows the changes in ion and electron temperature and density in a 2 minute interval.

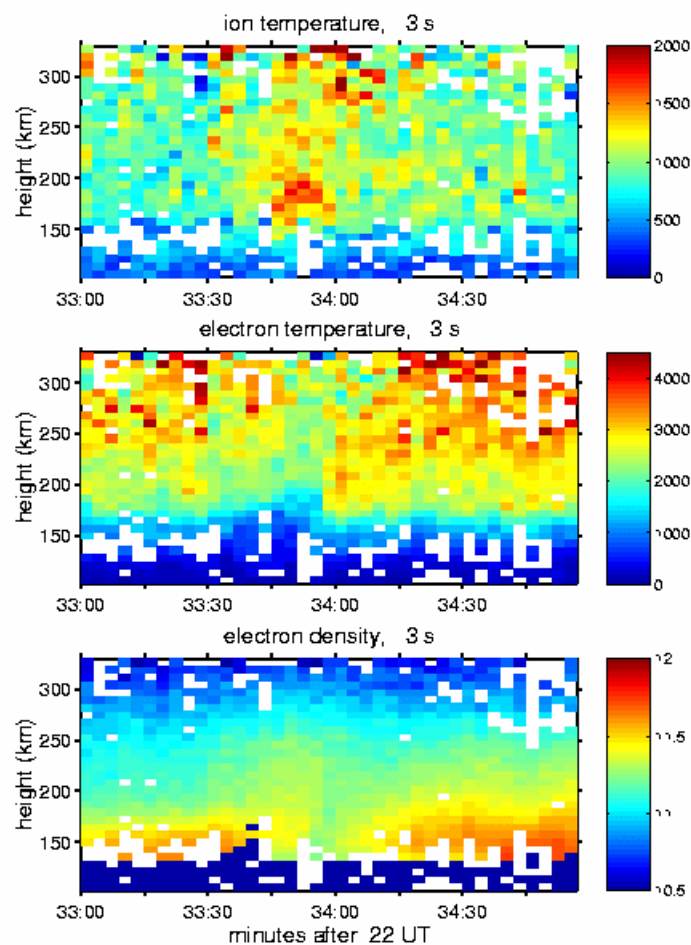


Figure 3 EISCAT UHF measurements from 28 January 1995 showing (i) an increase in ion temperature during 30 s before an arc enters the radar beam (ii) an increase in electron temperature immediately before the arc enters the radar beam and (iii) the rise in electron density in the F region as the arc fills the beam.

The increase in electron temperature occurs at 22:34 UT. Detailed modelling of this interval produces an excellent fit to the E region density, as seen in figure 4, where the time of the increase in T_e is marked with an arrow. In order to fit the profiles of T_e in this interval, however, it is necessary to include a heat source from ohmic heating.

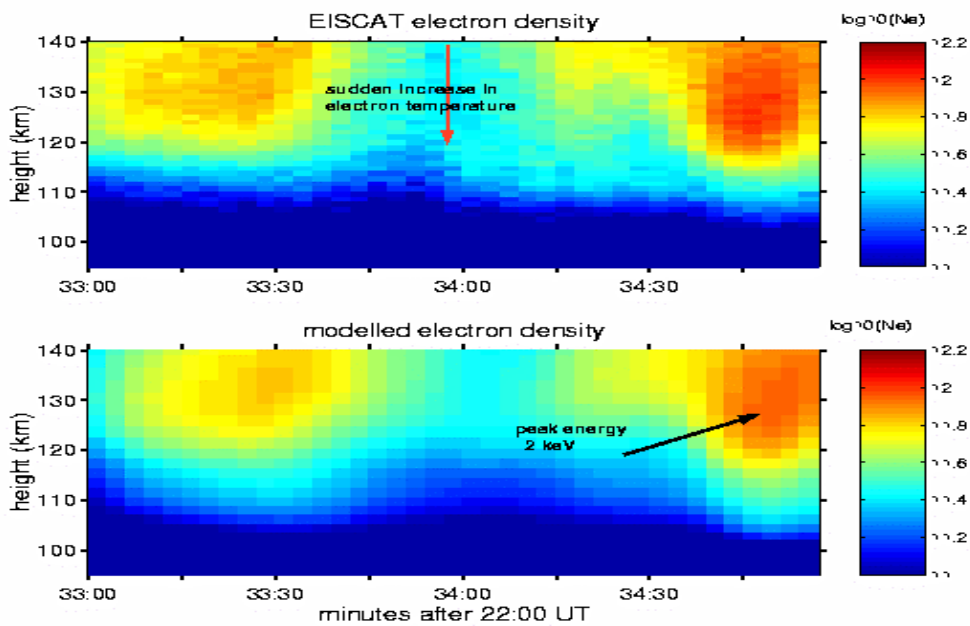


Figure 4 Electron density in the E region, measured and modelled. The increase in electron temperature occurs at the minimum of electron density.

The best fit, as seen in figure 5 requires field-aligned currents of $400 \mu\text{A m}^{-2}$ applied for only a few seconds (Lanchester et al., 2000). Other work that is proceeding in parallel with this is the development of a three-fluid simulation to study the electrodynamic consequences associated with ohmic heating by large field-aligned currents (Zhu et al., 2000). This work generates the time and space evolution of several electrodynamic quantities over a wider domain. This work confirms the result that the sudden increase in electron temperature beside an arc filament requires ohmic heating of electrons in a strong field-aligned layer.

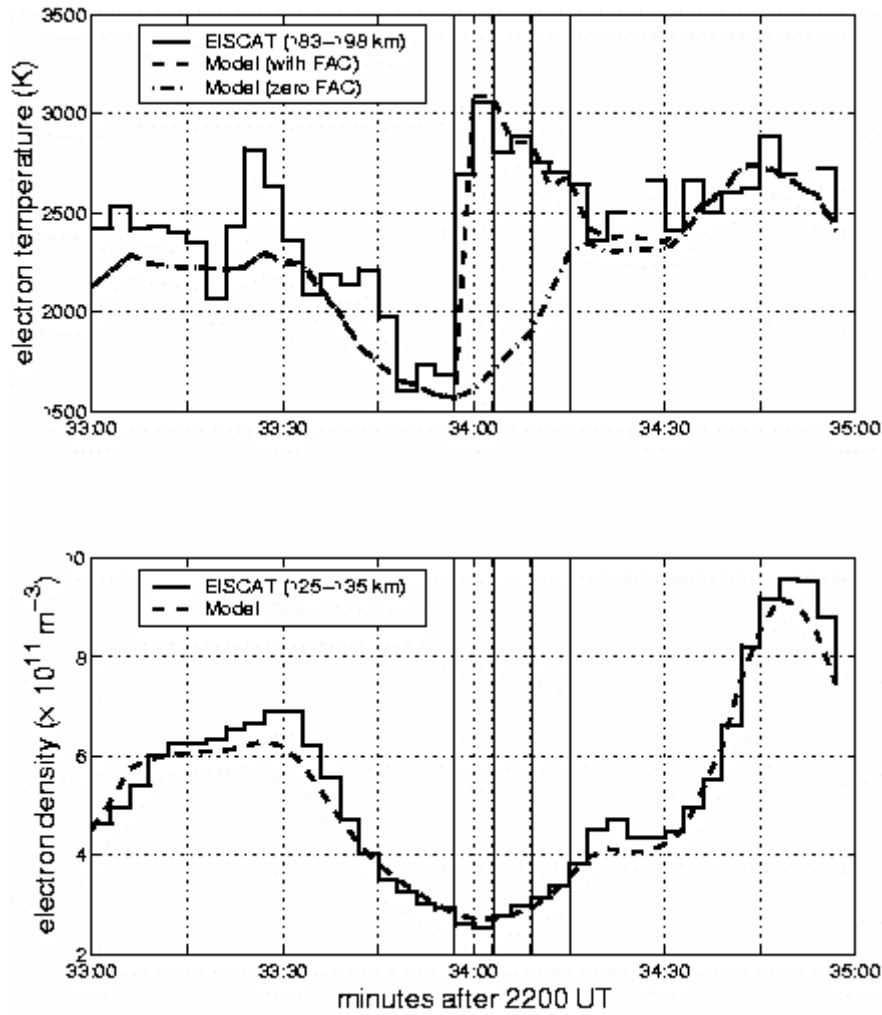


Figure 5 (top panel) Electron temperature in F region: measured by EISCAT (steps), modelled with heating from precipitation (dot-dash) and modelled with ohmic heating added (dash). (bottom panel) Electron density at peak of E region: measured (steps) and modelled (dash).

For the identification of magnetospheric acceleration processes, it is crucial to build up an understanding of the spatial and temporal morphology of the energy spectrum of the precipitating particles during geomagnetic storms. Collaboration between Lancaster University and MPAe (Max-Planck-Institut für Aeronomie) has enabled high-resolution energy maps of the particle precipitation to be produced. DASI (Digital All-sky Imager) and IRIS (Imaging Riometer for Ionospheric Studies) images give estimates of the particle precipitation of the soft electrons ($<10\text{keV}$) and hard electrons ($>25\text{keV}$), respectively. It is known that the ratio of absorption to the square root of optical intensity is an indicator of the energy for the precipitating electrons. EISCAT is able to make an accurate electron density profile measurement at one point within the common IRIS / DASI field of view. The energy spectrum of the precipitating electrons is computed by inverting the electron density profile measured by EISCAT. An exponential energy spectrum has been fitted to extract the characteristic energy. From this information high-resolution maps of the characteristic energy have been generated for the entire common IRIS / DASI field of view (figure 6).

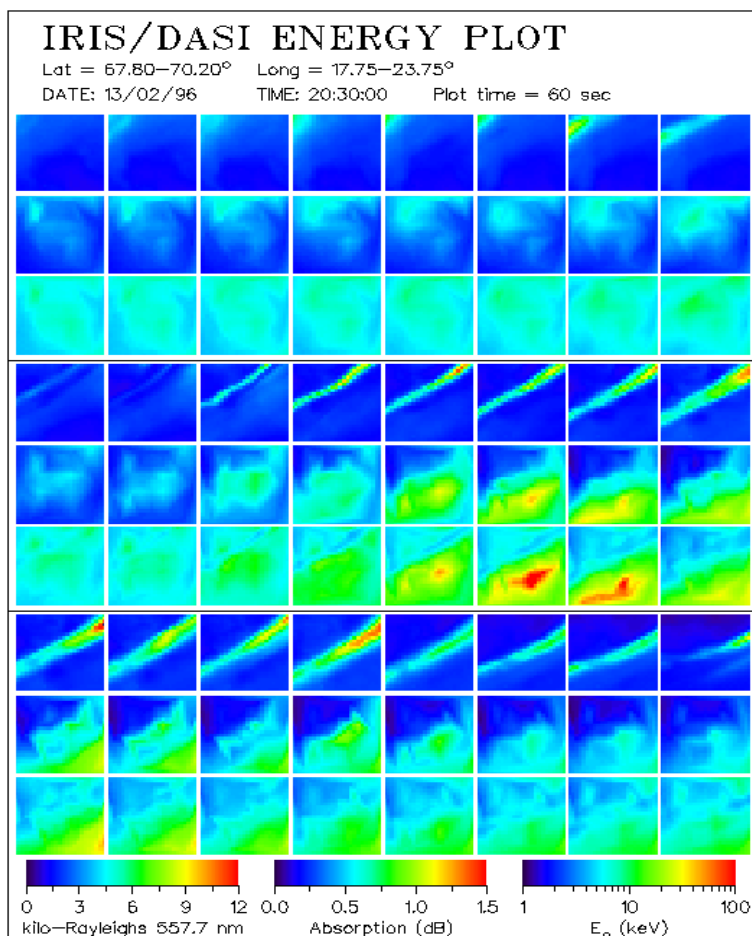


Figure 6 A time series, consisting of 3 sequential panels, showing DASI, IRIS and characteristic energy images. Each panel shows DASI optical images calibrated in Rayleighs at 557.7 nm (top in panel), IRIS absorption images calibrated in dB (middle in panel), and the characteristic exponential energy in key (bottom in panel). Each panel starts at 20:30 UT (top panel), 20:38 UT (middle panel) and 20:46 UT (bottom panel), stepping with 1 minute integration, on 13 February 1996. The field of view covered is 67.8-70.2 N° and 17.75-23.75 E°.

At the University of Sussex, further progress has been made in the analysis and interpretation of auroral observations in the nightside ionosphere, combining all-sky and narrow-angle data from Sussex imagers with data from the mainland EISCAT radar (e.g., Buchan, 1999). A major development has been the proposal of a new mechanism for interpreting and predicting the motion of auroral arcs in the nightside ionosphere during the expansion phase of a substorm. This was the result of work done in collaboration with colleagues at the State University of St. Petersburg.

The proposed mechanism combines the main ingredients of Petschek-type reconnection models (the MHD shock waves and their associated field-aligned currents) with those of auroral arc theories (the upward field-aligned currents associated with electrons precipitating into the ionosphere) and near-Earth acceleration mechanisms such as double layers to achieve the required energisation. The new feature in this interpretation is the proposition that the location and motion of auroral arcs observed during the expansion phase of a substorm, correspond to the ionospheric manifestation of upward field-aligned currents induced by earthward-propagating shock waves. These are generated during one or more reconnection pulses in the vicinity of an X-line in the magnetotail current sheet (figure 7). The delay between the onset of reconnection and the appearance of auroral arcs, reported in several publications, can then be explained in terms of the finite propagation speed of the shock waves as they travel from the reconnection site in the magnetotail to the ionosphere. The non-uniform plasma medium in the magnetotail leads to dispersion of the shock waves, resulting in poleward and/or equatorward moving auroral arcs.

This rich variety of behaviour provides a new framework for interpreting breakup arcs, and shows that their behaviour merits close examination.

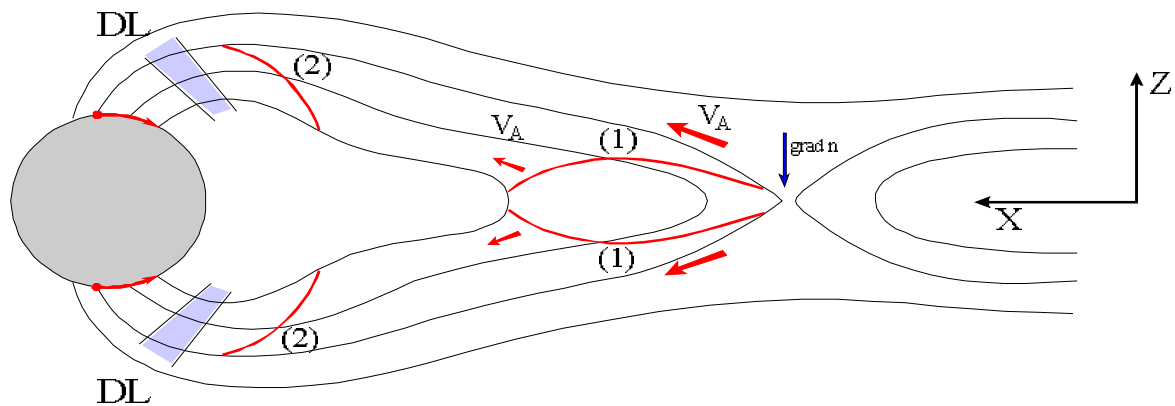


Figure 7 Simplified sketch showing the new mechanism for interpreting auroral arc motion during the substorm expansion phase. Reconnection at a near-Earth X-line generates pairs of shock waves propagating earthward and tailward. The earthward-propagating shocks are shown at two different times, labelled (1) and (2). The shape of the wave fronts changes with time because the waves propagate at the local Alfvén velocity, which depends on the coordinate perpendicular to the current sheet, z . The shaded region in the near-Earth magnetosphere, labelled DL (double layer) represents a region with a field-aligned potential drop, in which charged particles are accelerated into the ionosphere. The precipitating particles give rise to discrete auroral arcs, the motion of which reflects the arrival time of different parts of the shock fronts.

To analyse and predict the arc dynamics resulting from this mechanism, the Sussex group has developed a simple model which incorporates a time-varying reconnection process, and takes into account the non-uniform nature of the magnetotail plasma medium through gradients in the number density perpendicular to the central magnetotail current sheet. Analytical and numerical studies of this model reveal that:

- The morphology and location of the arcs is strongly dependent on three parameters: the plasma density distribution in the magnetotail, the position of the X-line, and the behaviour of the reconnection rate.
- Poleward moving arcs appear preferentially when the reconnection-generated shocks arrive quickly in the near-Earth magnetosphere, they sample weak gradients in the magnetic field and plasma density, and hence the Alfvén velocity, and the reconnection electric field is weak.
- Equatorward moving arcs occur preferentially when the shocks take a long time to arrive, gradients in the magnetic field and plasma density are strong, and the reconnection electric field is strong.

Comparison of the results obtained from simple numerical simulations of auroral dynamics with actual observations of substorm intervals recorded at Tromsø show that the proposed model could explain the complex structure and dynamics associated with auroral intensifications (figure 8).

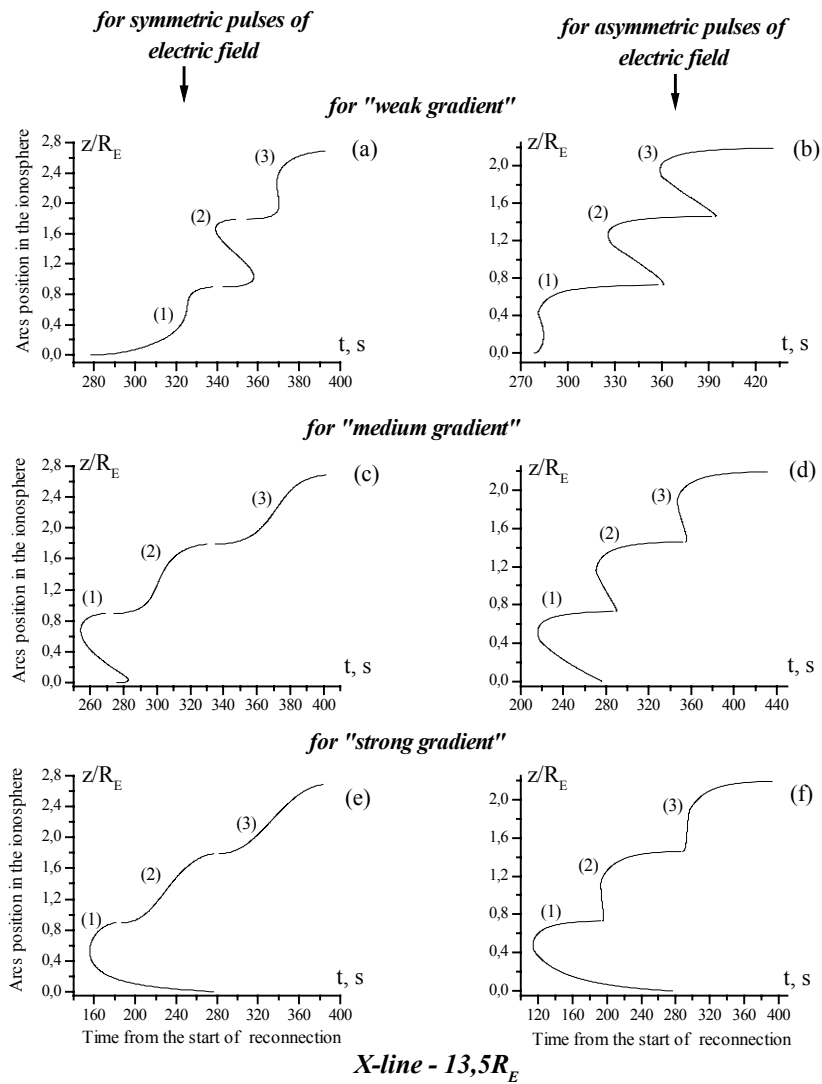


Figure 8 Results obtained from the simulation of auroral arc dynamics using various model parameters. These form a possible interpretation for a “mini breakup” recorded at Tromsø on the 18th February 1993 at 22:35 UT; keogram data for which is available at www.susx.ac.uk/physics/research/space/spghmp.htm.

All panels show latitudinal variations of auroral arcs as a function of time for various model parameters. The left panels (a), (c), and (e) show model results for three symmetric pulses of the reconnection electric field, and the right panels (b), (d), and (f) for three asymmetric pulses of the electric field. The top panels (a) and (b) were obtained for a weak spatial plasma density gradient, the middle panels (c) and (d) for a medium spatial plasma density gradient, and the bottom panels (e) and (f) for a strong plasma density gradient. These results were obtained for an X-line located at 13.5RE downtail, estimated as the location mapping to the Tromsø observations using the Tsyganenko T89 model. The lower panels, corresponding to a strong plasma gradient, reproduce the observations best.

The Southampton group was the first in the UK to publish a full-scale study based on data from the EISCAT Svalbard Radar. Sedgemore-Schulthess et al. (1999) have shown naturally enhanced ion-acoustic spectra from the vicinity of the dayside cusp/cleft associated with small-scale, dynamic auroral forms of order 100 m and less in width. Figure 9 shows coherent spectra from one 10-s dump of the gup0 experiment together with a corresponding narrow-angle camera image displaying a coronal auroral form, similar to those seen during all the enhanced spectra events detected, and not seen at any other time. The hatched circle in the auroral image represents the position and size of the ESR beam. Naturally enhanced ion-acoustic spectra are most commonly interpreted as being due to plasma turbulence driven by short bursts of intense field-aligned current, somewhat analogous to a lightning discharge. Observed previously with the Millstone Hill and EISCAT KST systems, observations of such spectra are commonly associated with precipitation boundaries, but in more general terms they indicate the presence of sharp conductivity gradients. The latest study shows evidence that enhanced spectra events correlate with poleward-moving auroral transients, indicating a possible association with time-varying magnetopause reconnection. Enhanced ion-acoustic spectra and their interpretation are the subject of a review article by Sedgemore-Schulthess and St.-Maurice (submitted to *Surveys in Geophysics*).

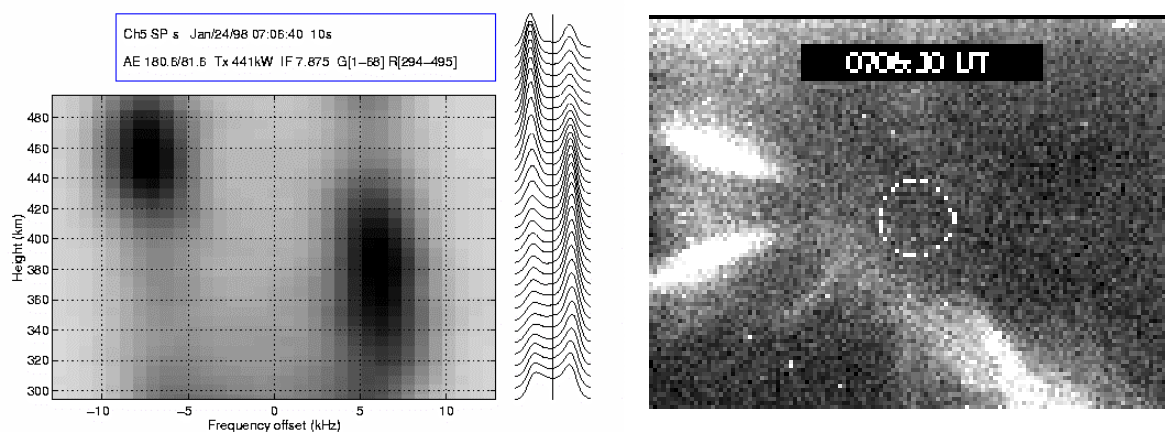


Figure 9 Naturally enhanced ion-acoustic spectra from the EISCAT Svalbard Radar (left), and a simultaneous narrow-angle auroral image (right) with a 16x12 degree field-of-view and a resolution better than 100 m. Enhanced ion-acoustic spectra are most likely due to either streaming plasma instabilities, due to field-aligned currents of order 1 mA m^{-2} or weak Langmuir turbulence. Such spectra occur typically as transient events and are correlated with discrete and dynamic auroral structures. The hatched circle in the auroral image represents the position and size of the radar beam.

The ESR data referred to above were collected during a campaign in January 1998 in which the CAPER sounding rocket was scheduled to fly. Owing to technical problems the CAPER flight, the purpose of which was to investigate of the cleft ion fountain (CIF), took place instead in January 1999. The UK contributed 40 of the 100 hours of EISCAT (ESR and VHF) time allocated to the experiment, the total being shared between the UK, Norway, Japan and Sweden. The EISCAT campaign achieved its main objective in covering the successful launch of the CAPER rocket from the Andøya range at 0613 UT on 21 January 1999, and high quality gup3 data were collected. Long pulse data covering the launch period are shown in figure 10. Meridian scanning photometer data show the ESR sitting just to the north of the open-closed field line boundary at the time of the launch, and the rocket reached apogee over Svalbard at the end of the large ion outflow event seen between 0615 and 0620 UT.

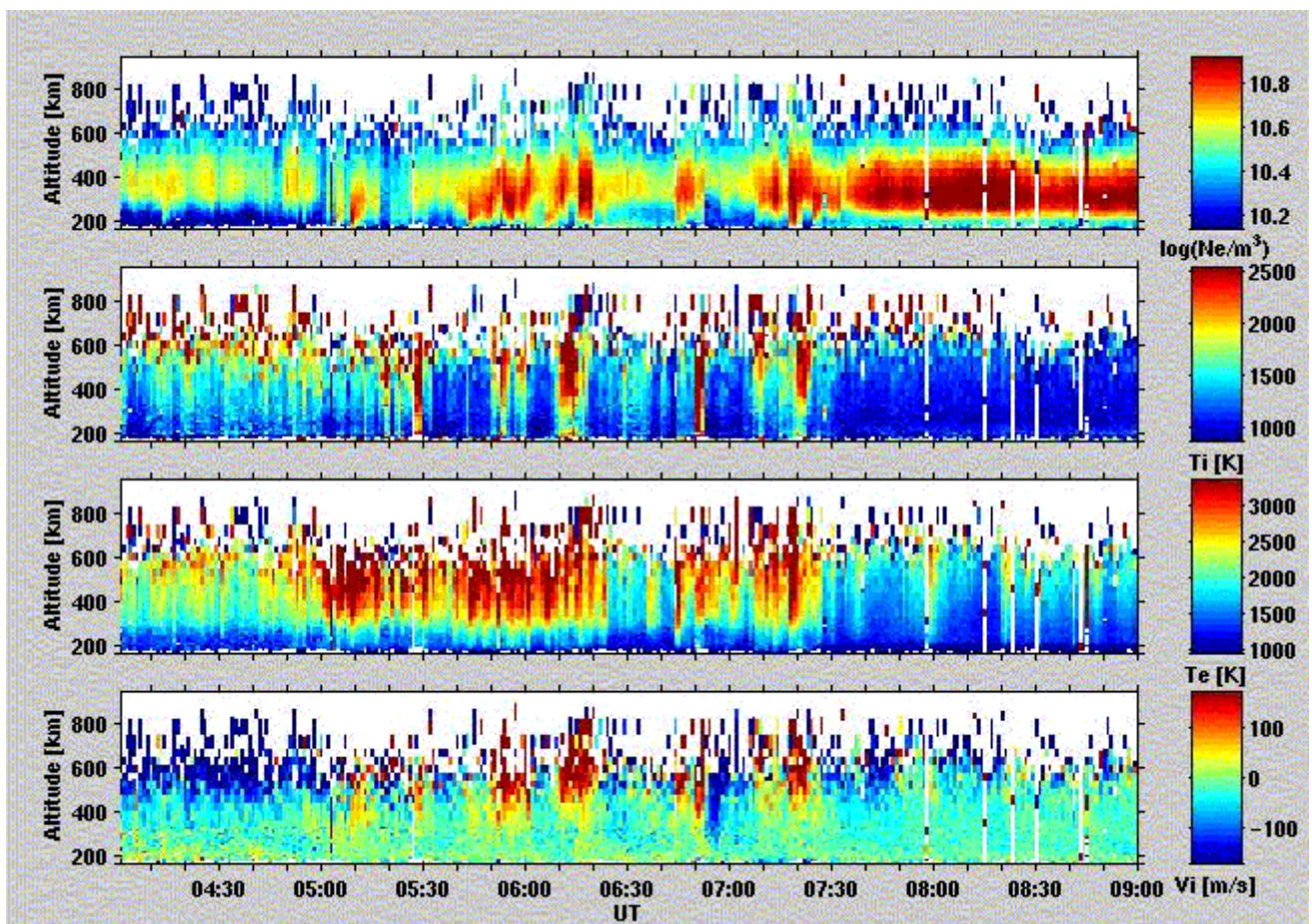


Figure 10 EISCAT Svalbard Radar long pulse data covering the CAPER launch period on 21 January 1999. The panels, from top to bottom, represent electron density, ion temperature, electron temperature, and ion velocity (positive away from the radar). The CAPER rocket, part of a campaign devoted to a study of the Cleft Ion Fountain, was launched at 0613 UT during a major ion outflow event.

6. Instabilities

Researchers from the University of Lancaster undertook a successful experiment in December 1998 during the UK EISCAT campaign in collaboration with MPI Lindau. The campaign aimed to investigate the auroral absorption during E-region instability conditions. The comparison of the 2D images from IRIS and STARE (Scandinavian Twin Auroral Radar Experiment) observations during FB (Farley-Buneman) instability conditions indicated that the absorption of cosmic noise in the D-region is dramatically reduced during periods of strong electric field enhancements (figure 11). This appears to be due to the development of a strong ion-acoustic turbulence, over a very large band of wavelengths, perpendicular to the magnetic field, and a resultant screening of the penetration of both the precipitating particles and cosmic noise into the D-region. This anti-correlation of absorption with electric field has also been observed in a recent study of a CME (coronal mass ejection) event on 10 January 1997 (del Pozo *et al.*, 1999).

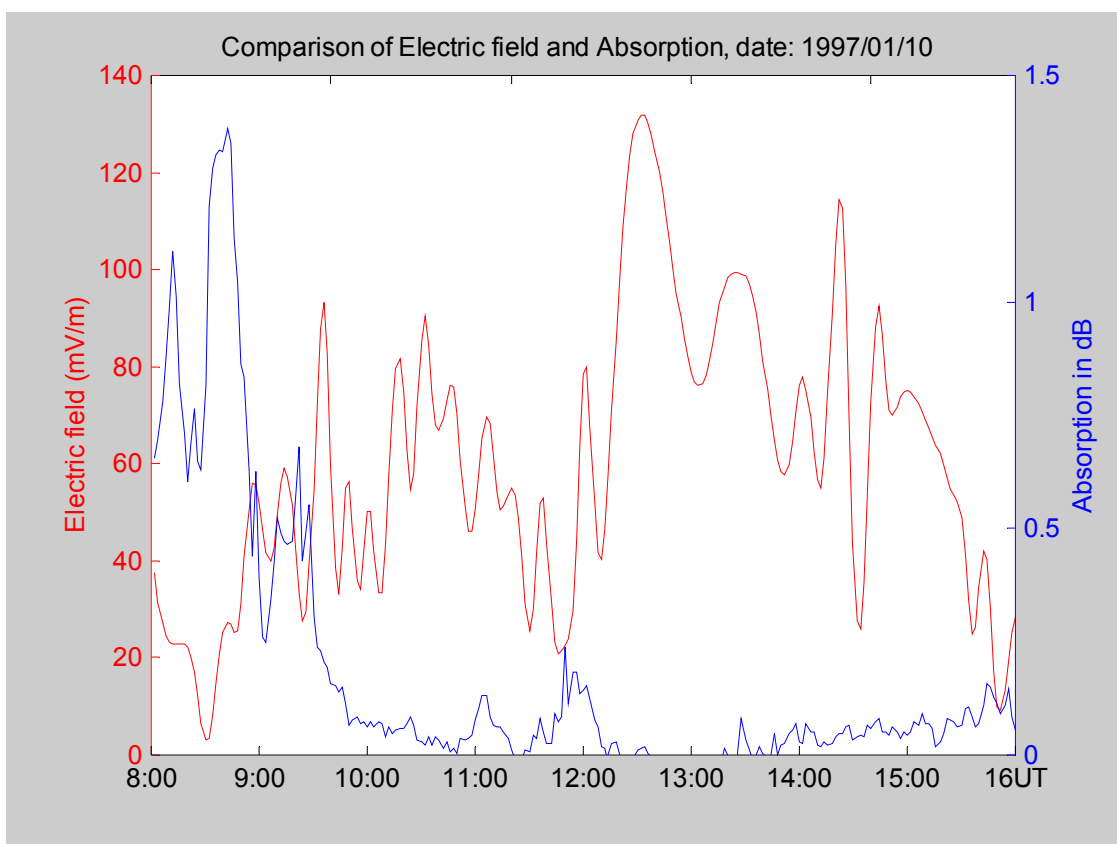


Figure 11 EISCAT measurement of electric field (red) and IRIS observation of ionospheric absorption (blue) as a function of time during the CME event on 10 January 1997, indicating the anti-correlation between absorption and the electric field.

7. Electrodynamicics

In conjunction with the IMAGE magnetometers IRIS has been used for the study of small-scale and short-lived current vortices observed in the evening sector. The electric fields, conductances and horizontal currents as well as particle spectra have been measured by EISCAT. All-sky cameras obtain optical signatures of these vortices, while IRIS provides information on the associated energetic particle precipitation. Preliminary studies indicates that the current vortices are produced by ionospheric Hall currents which encircle flux tubes containing upward and downward field-aligned currents.

The electrical conductivity of the ionospheric plasma governs the extent to which currents flow in the ionosphere in response to electric fields, the latter principally of magnetospheric origin. The EISCAT UHF radar is unique in its ability to provide simultaneous observations of the electric field, yielded by the F-region tristatic velocity measurements, and estimates of the conductances – the height-integrated conductivity – to which electron densities in the lower ionosphere principally contribute. The interrelationship between the electric field and particle-produced Hall and Pedersen conductances, was investigated statistically by Davies and Lester (1999). Results based on some 1300 hours of field-parallel observations from CP-1 and CP-2, revealed that in general the times of peak conductance identified from the entire set of EISCAT observations, do not correspond to the times of the largest electric field values. The relative contribution of ionospheric conductance and electric field to the electrojet currents therefore depends critically on local time. The tendency for a decrease in both Hall and Pedersen conductances, accompanied by an increase in the electric field, at least for moderate and large electric field values, is also identified to some extent in the ratio of the conductances, thus acting as an indicator of the energy of precipitating particles.

8. Ionosphere-Thermosphere Interactions

Ion frictional heating, in response to imposed electric fields, constitutes one of the principal mechanisms whereby energy originating in the solar wind is deposited into the ionosphere and ultimately the neutral atmosphere. In a continuation of previous work by the authors, Davies et al. (1999a) investigated the solar and seasonal dependence of ion frictional heating, based on an extensive database of EISCAT UHF common programme observations, which extended over an entire solar cycle, solar cycle 22. Ion frictional heating was found not to increase significantly between solar maximum and solar minimum, which was contrary to what was expected by examination of the corresponding variation of ion velocity. This was explained with respect to a number of other competing factors, which acted to suppress frictional heating under solar maximum conditions. Seasonal effects on the diurnal distribution of ion frictional heating are well explained by corresponding variations in ionospheric convection, the latter principally a result of geometrical factors.

Ion frictional heating was found to be a significant factor in the generation of topside auroral ion upflows in an earlier statistical study by Foster et al. (1998). In addition to their use of CP-1 and CP-2 observations the authors employed an exhaustive set of common programme 7 (CP-7) observations from the EISCAT VHF radar which enabled investigation to be extended up to 800 km in altitude. Upflow events were identified as exceeding predetermined thresholds in either upward plasma flux or velocity or indeed both. Analysis revealed that the number and nature of upflow events varied not only diurnally but also with season and solar cycle. One interesting conclusion was that whilst ion upflow events identified by the velocity selection criterion tended to predominate at solar minimum, under solar maximum conditions, events characterised by large upward ion flux were dominant. Between 50 and 60% of upflows occurred simultaneously with enhanced ion temperature and some 80% were associated with an enhancement in either ion or electron temperature.

At University College, London, work has commenced on investigating the so-called "Flywheel Effect" in ionosphere-thermosphere coupling. This comes about when sudden change occurs in ion flow in the auroral zone. If a large electric field is suddenly imposed, as during a sudden storm commencement, or alternatively fast ion flows are turned off as the driving potential is cut, the situation can arise where instead of the ions driving the neutrals, the neutral wind continues under its own momentum and starts to "drive" the ions. The result can be significant feedback into the magnetosphere, and a reversal of the "usual" direction of energy flow. This work grew out of a consideration of the effects of geomagnetic history by Aruliah et al, where it was shown that the failure to consider the inertia of the neutral wind could result in significant mis-estimates of the Joule heating occurring in polar cap and auroral zone. Modelling using the UCL-Sheffield CTIM model shows that at times of large variability in magnetospheric input, failure to take into account the neutral atmosphere response can lead to underestimates of up to 50% in the Joule heating - even in specific locations up to 100%.

Neutral wind data has been used from the UCL FPIs as part of a study of the airglow seen during Heater experiments. Work with Björn Gustavsson and others at the IRF in Sweden has considered whether the difference in location between Heater input and airglow volume could be due to thermospheric wind drift, and a paper is in preparation. Ion-neutral coupling studies continue with comparisons between the UCL FPIs and the radars. The contribution of E-region winds to the energy balance in theta aurorae is being studied with a plan for a series of observations with the UCL FPIs. The FPIs will observe 557.7 nm airglow as part of a combined study with STARE, magnetometers and other instrumentation as a test of a new modelling technique by Amm et al.

A considerable fraction of the solar wind energy that crosses the magnetopause ends up in the high-latitude thermosphere-ionosphere system as a result of Joule heating, the consequences of which are very significant and global in nature. Often Joule heating calculations use hourly averages of the electric field, rather than a time-varying electric field. This leads to under-estimates of the heating. Researchers at the University of Sheffield have determined the magnitude of the under-estimate of Joule heating by analysing EISCAT electric field data. Plasma velocity observations from the field-aligned position from Common Programme 2 were used, giving 745 hours of data collected over a four-year period from February 1987 through to February 1991.

The Sheffield group find that the under-estimate due to using hourly-averaged electric field values is 20%, and with a upper value of about 65%. They show that these values are remarkably insensitive to changes of solar flux, magnetic activity and magnetic local time. A coupled ionosphere-thermosphere model has been used to calculate the local changes these under-estimates in heating rate cause to the neutral temperature, mean molecular mass and meridional wind. These changes are each in the order of a few percent. These variations cause a reduction in the peak F-region concentration of 20% in the summer hemisphere at high latitudes, and about half this level in the winter hemisphere. The Sheffield group have suggested that these calculations could be used to add corrections to modelled values of Joule heating.

9. Large-Scale Structure

The complementary roles of the EISCAT radars and radio tomography have been exploited in multi-instrument studies at the University of Wales, Aberystwyth that have led to advances in both the tomographic technique and the understanding of solar-terrestrial coupling processes. Electron densities measured by the mainland EISCAT radar have been central in the development and validation of tomographic reconstruction methods (Spencer et al., 1998; Bernhardt et al., 1998), and have yielded test cases including extreme ionospheric conditions for comparisons of inversion algorithms (Pryse et al., 1998a). The comparisons have demonstrated that reliable tomographic images can be obtained for a wide range of ionospheric distributions, provided that appropriate *a priori* information is used for the reconstruction process.

The EISCAT mainland radar was used in experiments providing insight into the physical processes responsible for the dayside high-latitude trough (Pryse et al., 1998c). Geomagnetic conditions were extremely quiet for most of the time interval of interest, but activity increased dramatically towards the end. Tomographic images covering a wide range of latitudes revealed the trough to be persistently at high latitudes during the quiet period, but then migrating to lower latitudes with increasing activity. The results were interpreted in terms of the polar-cap plasma convection pattern with the trough in the return sunward flow. Increased ion temperatures measured by the EISCAT radar during the disturbed conditions demonstrated that ion frictional heating gave rise to a very deep trough in the late-afternoon sector.

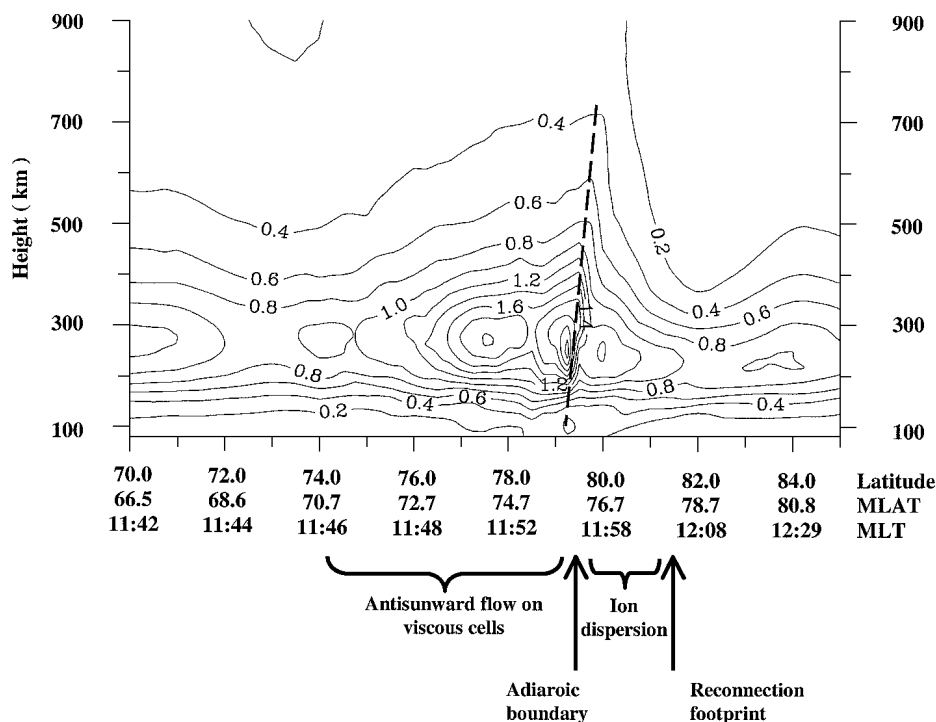


Figure 12 Tomographic image for a NIMS satellite pass at 0845 UT on 21 January 1998 showing contours of electron density (10^{11} m^{-3}) (Pryse et al., 2000).

Complementary observations made by radio tomography and the ESR and CUTLASS radars were used to link a latitudinally-narrow field-aligned density enhancement with a temporally confined enhancement measured by ESR in a region where the HF radar indicated low-velocity sunward components (Mitchell et al., 1998).

In a multi-instrument study under steady northward IMF, measurements made by six complementary experimental techniques including radio tomography, ESR, all-sky and meridian scanning photometer auroral optics, HF coherent scatter radar and satellite particle detectors, revealed plasma parameters consistent with lobe reconnection (Pryse et al., 2000). Each of the instruments individually provided valuable information on limited aspects, but taken together the different experiments complemented each other to give a comprehensive picture of the dayside ionosphere. The ESR electron densities (figure 13, top panel) affirmed the density distribution of the tomographic image (figure 12), showing a steep gradient with densities increasing to the south at the adiarocic boundary. Increased electron temperatures observed by ESR (figure 13, centre panel) were consistent with precipitation within the region of reverse ion-dispersion. The line-of-sight velocities (figure 13, bottom panel) revealed a tendency for F-region flows to be towards the radar over the entire field-of-view, with the exception of a narrow latitudinal band just north of the radar. This was consistent with the CUTLASS observations and with the general pattern expected under $B_z > 0$ of sunward flow in the polar-cap lobe cell with anti-sunward flow associated with viscous cells at lower latitudes.

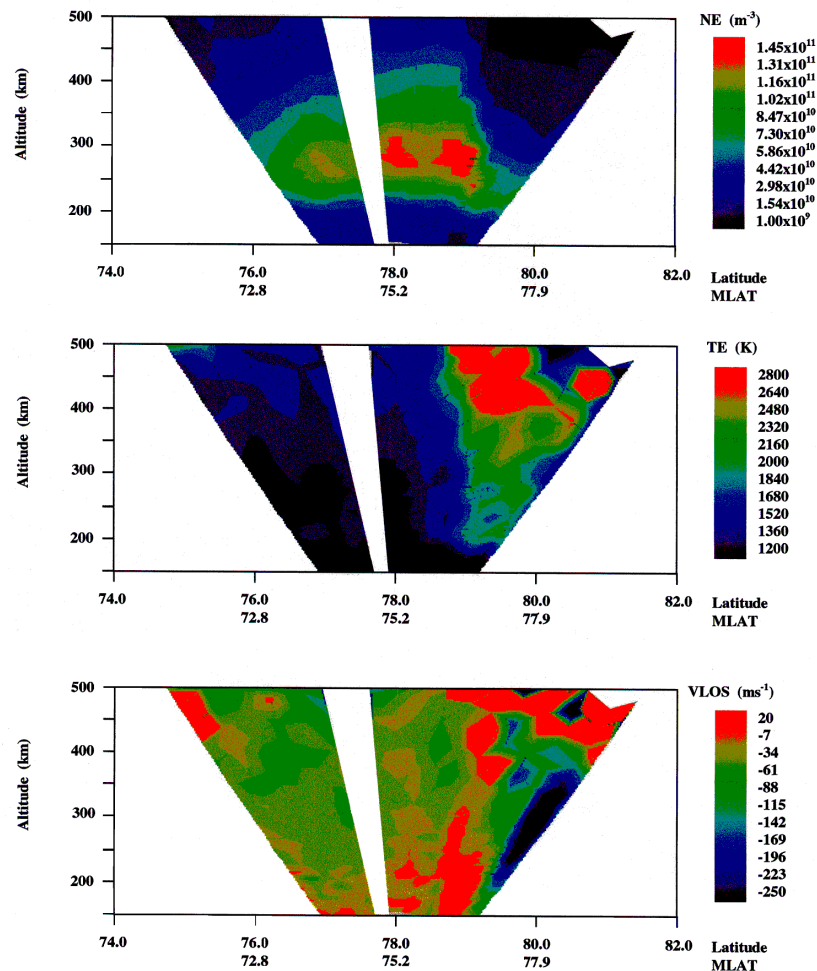


Figure 13 Electron densities (top panel), electron temperatures (centre panel) and line-of-sight ion drift velocities (bottom panel) measured by the ESR radar during a scan in the magnetic meridian between 0830 and 0900 UT on 21 January 1998 (Pryse et al., 2000).

The Tromsø Dynasonde is a digital ionosonde measuring the amplitude and phase of radio echoes reflected from the ionosphere. In addition to the frequency and virtual range of each echo, one parameter of particular interest is the direction-of-arrival, which allows horizontal structures in the ionosphere to be studied. Under suitable ionospheric conditions, where structures or strong gradients are present in the electron concentration, echoes may be observed out to horizontal distances of several hundred kilometres. In collaboration between RAL and BAS, Jones et al (2000) have developed a method for latitudinally mapping these gradients in F-region peak electron concentration using the Dynasonde. A comparison with the co-located EISCAT UHF radar shows good agreement lending credibility to observations of electron concentration gradients by a Dynasonde alone. This is significant because although EISCAT itself only runs on a campaign basis, the Dynasonde operates routinely throughout the year, making soundings every six or twelve minutes.

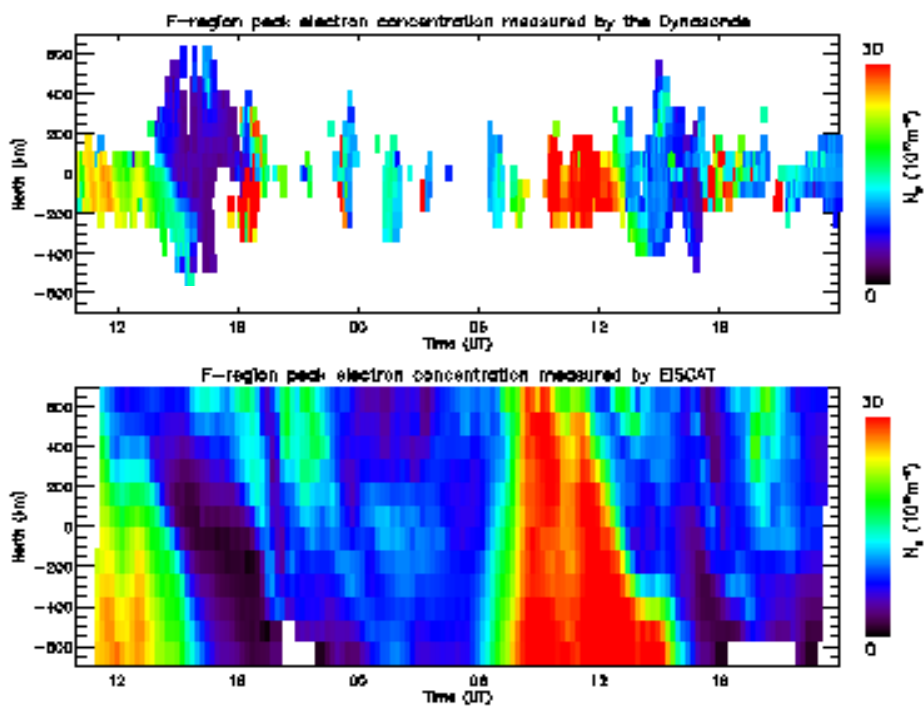


Figure 14 Upper panel: estimates derived from measurements made by the Dynasonde. Lower panel: measurements made by the EISCAT UHF radar running the CP-3 common program.

Figure 14 shows results from a comparison of F-region peak electron concentrations on 9th and 10th November 1993. The upper panel shows estimates derived from measurements made by the Dynasonde; the lower panel shows measurements made by the EISCAT UHF radar running the CP-3 common program. The overall agreement between observations from the two instruments is very good indeed. Not only is the Dynasonde able to detect broad features such as the diurnal maxima and minima, but when off-vertical echoes are received, it is possible to track the evolution of features as they move with latitude or change with time. A particularly good example of this is the edge of the trough and its associated gradient, which moves southward between 14 and 16 UT on the 9th. Such a strong gradient provides suitable propagation conditions for the Dynasonde signals to be received from directions well away from the vertical. When such conditions exist, the Dynasonde is able to map the peak electron concentration over distances up to several hundred kilometres north or south, an impressive achievement for a routine sounding technique. An advantage of the Dynasonde is that a single sounding only takes a few minutes to complete compared with the thirty minutes that EISCAT takes to return to the same

position in its meridian scan. The better time resolution of the Dynasonde illustrates how a comparative study between the two instruments has the potential to deconvolve spatial and temporal changes in the electron concentration. New sounding methods developed using the Tromsø Dynasonde are reported by Wright and Pitteway (1999).

A statistical comparison of ion and electron temperatures and electron densities measured using the Tromsø UHF and ESR radar has been undertaken at Sheffield Hallam University. This is the first time that data from the ESR has been used for a statistical study. The data set used was the field aligned gup0 observations from March 1996 to August 1998 and was compared to the observations from the Tromsø UHF radar during the same period. Histograms showing the distribution of the measured plasma parameters at a specified height were produced, as well as temporal distributions of enhanced ion and electron temperatures for each radar. The results from this study were presented at the 9th EISCAT international Workshop in Wernigerode, Germany. Figure 15a shows the temporal distribution of enhanced ion temperatures at an altitude of 3000 Km for the EISCAT UHF radar and figure 15b represents the corresponding distribution from the ESR.

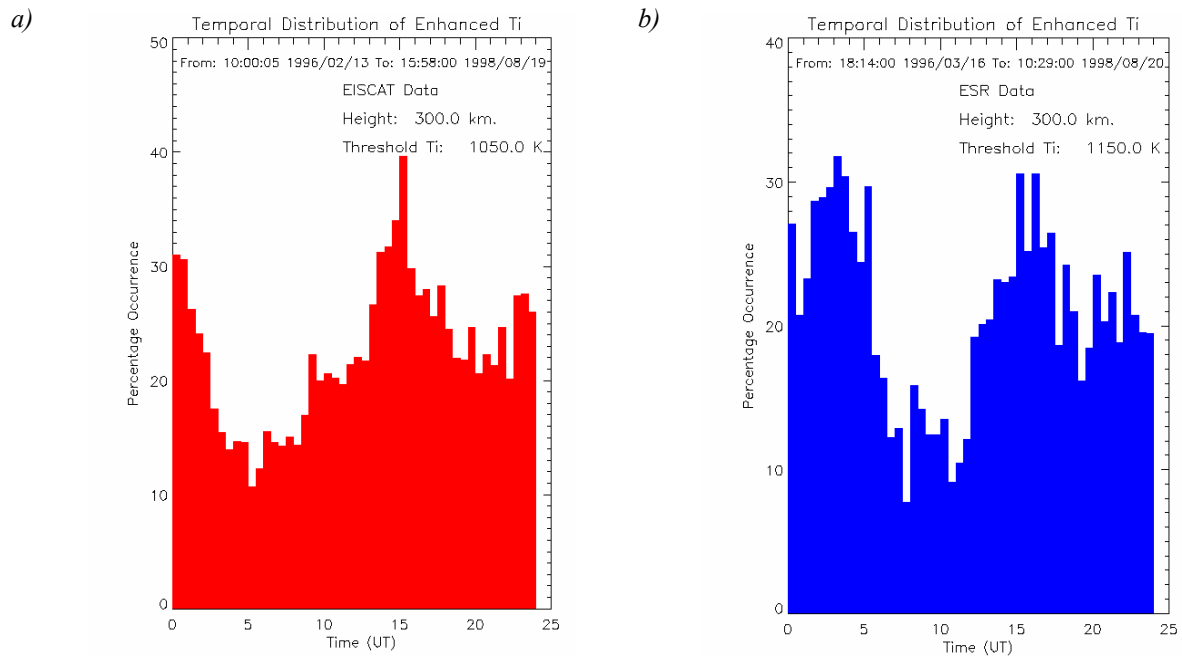


Figure 15 Histograms showing the temporal distribution of enhanced field-parallel ion temperatures: (a) as measured in the two-year EISCAT Common Programme data set, and (b) in ESR data as deduced from the two year ESR (GUP0) data set.

The results from figure 15a have previously been discussed by McCrea et al and Davies et al and show two distinct peaks with a minimum in the occurrence around 10UT on the dayside and centred on 19UT on the nightside. By comparing this to figure 15b, it can be noted that the distribution is also double peaked, but the peaks are displaced in time relative to their occurrence at Tromsø. The minimum in occurrence of enhanced ion temperatures at ESR is not as clearly defined as EISCAT due to the suggestion of a subsidiary peak around 9UT. Figure 16a shows the temporal distribution of enhanced electron temperature at EISCAT UHF, while figure 16b shows the comparative distribution at ESR. The Tromsø distribution shows low occurrences on the nightside with a peak on the dayside, while ESR has a double peaked distribution. Some of these observations can be explained due to the difference in location of the two sites. Further investigations are currently underway to identify further explanations.

Another study being carried out at Sheffield Hallam involves the identification of anomalous incoherent scatter spectra. Such asymmetric spectra seem to occur only in ESR data, and it is these data that are being targeted in the search.

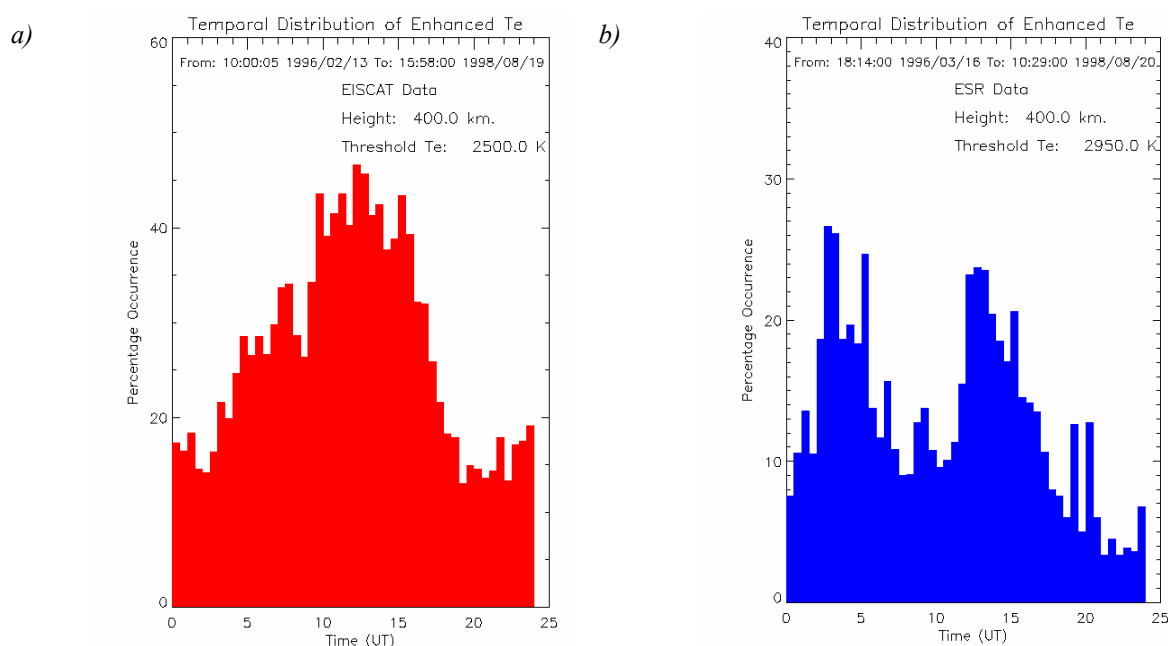


Figure 16 As for figure 15, but for enhanced electron temperatures

10. Artificial Heating

On 16 February 1999, during a joint heating campaign involving the UK (University of Lancaster), Germany and Sweden, enhanced airglow at 6300 Å was observed by HF pumping the ionospheric F region plasma at auroral latitudes using the EISCAT Heating transmitter. The airglow was detected simultaneously by up to four imaging stations of ALIS in northern Sweden (figure 17). Airglow enhancement occurs as a result of excitation of the $O(^1D)$ meta-stable state, which radiates at 6300 Å (the red line) as the oxygen atom relaxes to its ground state. Two different mechanisms have been proposed for the excitation of the electrons and subsequent airglow enhancement. In the first case it is assumed that the electron velocity distribution remains essentially Maxwellian and the energetic electrons are associated with the tail of the velocity distribution of the pump-enhanced electron temperature. In the second case the supra-thermal electrons belong to a non-Maxwellian distribution, which results from acceleration processes in Langmuir turbulence driven by the pump. EISCAT observation indicates large heater-induced electron temperature enhancements of up to 4500 K, or 450% of the unperturbed temperature, which extend several tens of kilometers below and several hundreds of kilometers above the airglow cloud. The short vertical extent of the airglow cloud and the high anomalous absorption of the pump wave that is expected for the large electron temperature enhancements, suggest that the electron energisation needed to enhance the airglow occurs essentially perpendicular to the magnetic field and is due to upper hybrid turbulence.

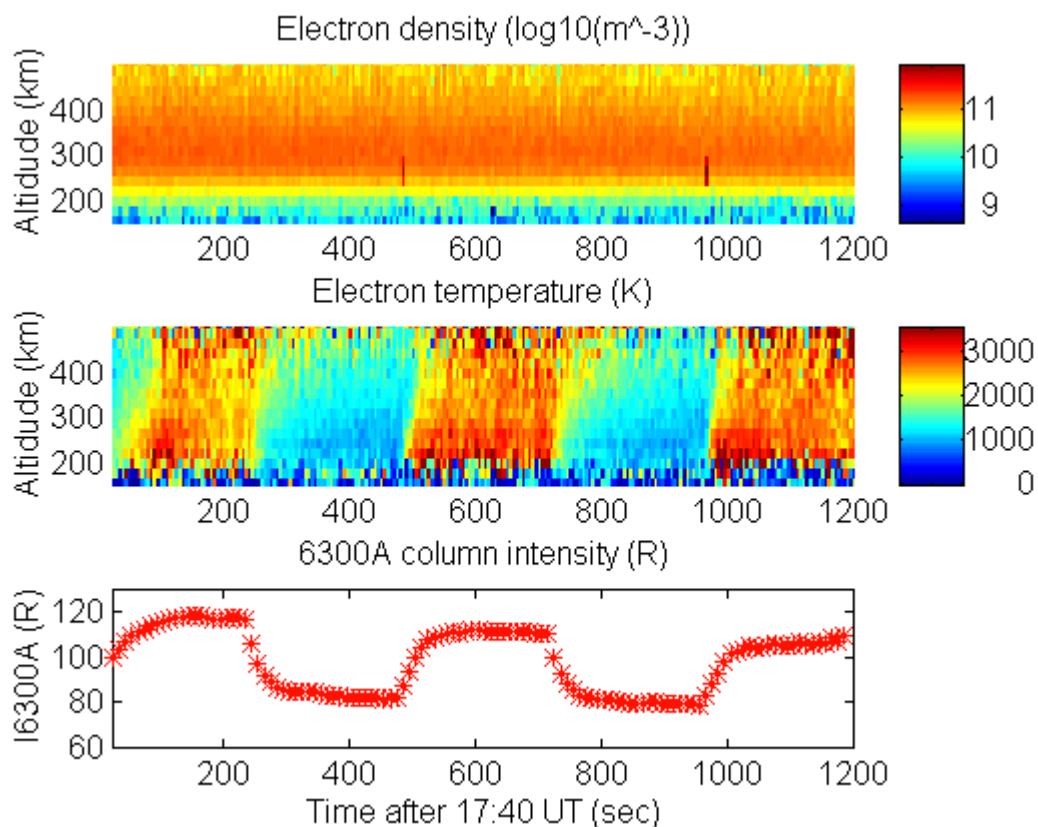


Figure 17 Electron density and electron temperature versus altitude as measured by EISCAT-UHF radar, and the 630 nm emission intensity measured with ALIS. The measurements were made during the ionospheric heating experiment on 16 February 1999.

Robinson et al. (1998a) presented results from artificial modification experiments in which the EISCAT heating facility was employed to modify the Hall current region of the auroral ionosphere while the electrojet was enhanced. During conditions characterised by a weak electrojet and completely underdense heating, electron temperature increases, as expected, were inferred from observations by the UHF radar at all altitudes between 100 and 135 km. However, under conditions of a strong electrojet and only slightly underdense heating, radar observations revealed that whilst above the electrojet – between 120 and 135 km – the electron temperatures were enhanced, in the altitude range 100 to 115 km RF modification appeared to actually reduced the electron temperature. These surprising results were discussed in terms of a theory of the interaction between high power electromagnetic waves and irregularities excited by the Farley-Buneman instability at electrojet altitudes. The spatial distribution of irregularities generated by the heater, and moreover their temporal development and motion, was diagnosed using the CUTLASS Finland radar by Robinson et al. (1998b). These results confirmed the crucial role played by field-aligned irregularity generation in heater induced anomalous absorption and electron heating. Stocker (1998) reviewed the special situation that arises when the heater is operated at a frequency near a harmonic of the electron gyrofrequency.

One of the key capabilities of the SPEAR radar, proposed by researchers from the University of Leicester, is the possibility of using its high power transmitter to inject waves and particles, via ionospheric modification effects, along geomagnetic field lines. This would allow an improvement in the co-ordinated study of magnetosphere-ionosphere coupling processes through the identification of common field lines between ground and space-based instrumentation. A feasibility experiment of such "field-line tagging" was performed using the EISCAT heater at Tromsø in collaboration with the FAST satellite. The first experimental attempts during the UK heating campaign of October 1998, succeeded in physically tracing a geomagnetic field line from the satellite at 2550 km altitude to within 10 km accuracy. It also enabled the location of the acceleration region of electrons responsible for field aligned currents passing along the common field line, to be identified as a point some 1000 km beyond the spacecraft. This result was obtained by modulating the heater at 3 Hz. The resultant 3 Hz modulation in the ionospheric conductivity induced a corresponding signature in field aligned current. This 3 Hz field aligned current was detected in the downward electron flux observed on board FAST and, moreover, a signal at that frequency was found in the electric field instrument and the upward ion flux detector on the spacecraft (see figure 18). Only a narrow region of 3 Hz modulated flux was detected by the spacecraft, which exactly corresponded to the size of the heated patch in the ionosphere, mapped along the geomagnetic field line. These results are reported in more detail by Robinson et al. (2000).

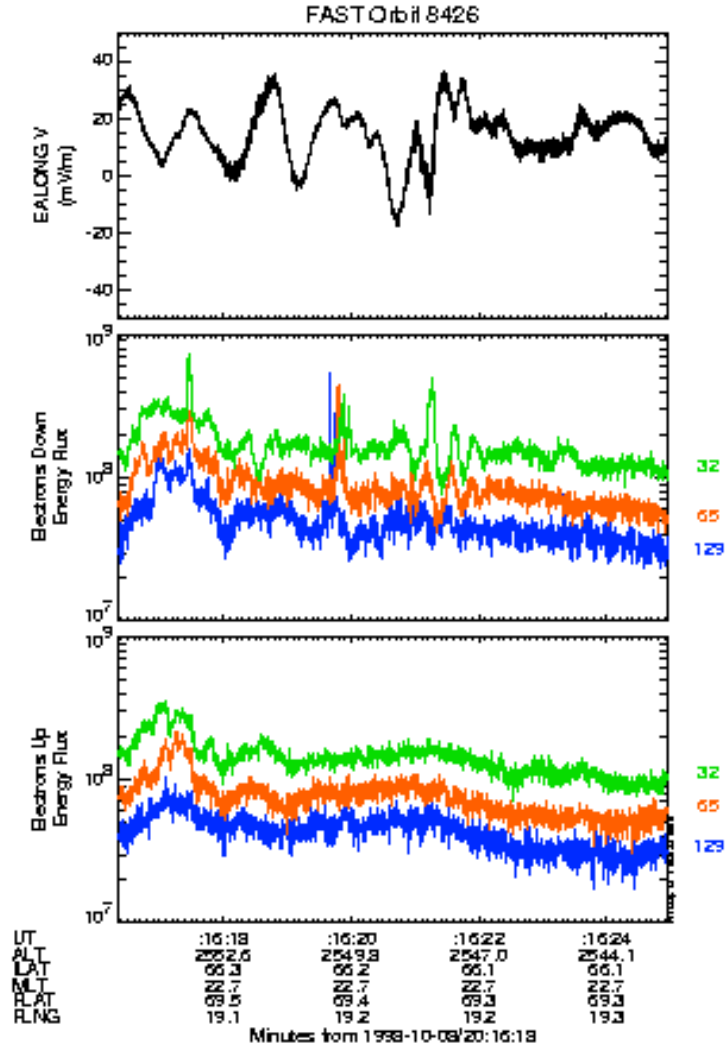


Figure 18 FAST observations from 8 October 1998 at around 20:16 UT. The uppermost panel illustrates the perpendicular electric field and the lower two panels present downward and upward magnetic field aligned electron fluxes, respectively. Between 20.16.19 and 20.16.23 UT, the signature of the 3 Hz ULF wave stimulated by the Heater is clearly visible in the electric field and down-going electron flux data.

11. ULF Waves

Observations of ULF waves with EISCAT are fairly rare, despite the fact that the EISCAT UHF radar can measure simultaneously with high accuracy the ULF wave electric field in the ionosphere and the E-region conductivity. Study of an interval of Pc5 activity on 21 April 1993, during which the EISCAT UHF radar operated in CP-1 mode, demonstrated that both of these parameters are important for generating ground-based magnetic signatures (Lester et al., 2000). This interval was divided into 3 distinct intervals, as shown in figure 19. In the first interval, no F-region signature of the pulsation was observed. There were clear perturbations, however, at the frequency observed in the ground magnetic signature of the wave, in the height integrated Hall conductivity, Σ_H , which pulsed between 10 and 60 Siemen. In interval II, whilst there were clear perturbations in the F-region electron density and electron and ion temperatures, as well as in the east-west component of the ion velocity (again at the same frequency as the magnetic signature) these were not evident in Σ_H . Moreover, the ion temperature enhancements led the electron density and temperature enhancements by 180°. The enhanced ion velocity associated with the ULF wave electric field caused the ion heating. The electron density and temperature enhancements were most likely caused by electron precipitation as a result of the ULF wave scattering electrons into the loss cone. The EISCAT observations during interval III were similar to those in interval I, with the signature of the Pc5 pulsation again confined to the E-region conductance.

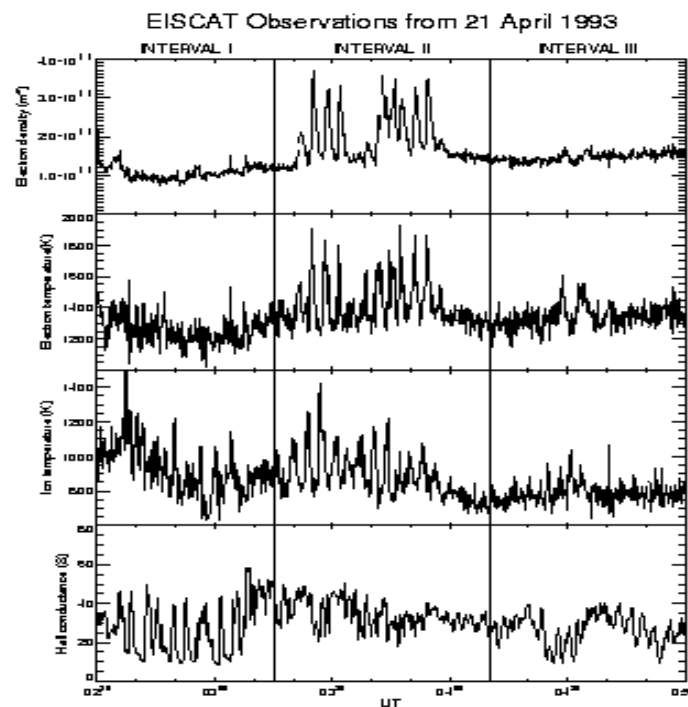


Figure 19 EISCAT CP-1 observations of F-region electron density, electron temperature and ion temperature between 0230 and 0500 UT 21 April 1993. The bottom panel illustrates the height integrated Hall conductivity derived during this interval from E-region power profile measurements.

Both the Leicester Doppler Pulsation Experiment (DOPE) and the EISCAT UHF radar observed a Pc5 wave on 13 February 1996. Tristatic flow measurements from the latter permitted direct verification of the Doppler technique for large scale ULF waves for the first time (Wright et al., 1998). This particular Pc5 was identified as being Alfvénic in nature - a so-called field line resonance. The work of Wright et al. (1998) confirmed that the Doppler signature produced by this type of wave is created by the vertical bulk motion of the ionosphere driven by the $\mathbf{E} \times \mathbf{B}$ drift associated with the pulsation electric and magnetic field perturbations. Moreover, and in contrast to the interpretations of previous low latitude results, the study indicated that waves at high latitude retain an Alfvénic character over a large spatial area.

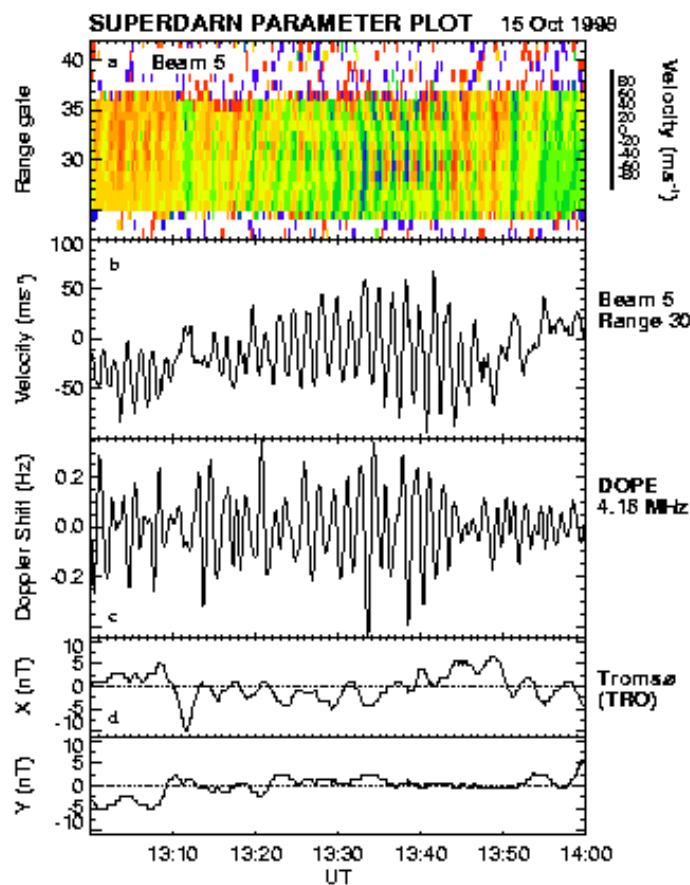


Figure 20 (a) Line of sight velocity data from beam 5 of the CUTLASS Finland radar as a function of range and time for the interval 1300-1400 UT on 15 October 1998. Also shown are the time series for (b) CUTLASS Finland beam 5, range 30, (c) DOPE frequency shift and (d) Tromsø (TRO) X- and Y-component magnetic field. The data from the DOPE sounder has been filtered to exclude periods outside the range 60-200 s.

The UK special programme SP-UK-OUCH employs the EISCAT high power HF heating facility at Tromsø to generate artificial field aligned irregularities, which produce high power backscatter observed by both the Iceland and Finland radars of the CUTLASS HF coherent scatter system. The coherent scatter radars are operated in a high spatial and temporal resolution mode, while the heater generates irregularities continuously over a period of several hours. The CUTLASS observations are supplemented by operation of the EISCAT mainland UHF radar. The artificial scatter can be turned on when natural irregularities are not present, enabling the observation of background geophysical processes at will. Both large-scale field line resonances and small scale particle-driven ULF waves can be observed in this way. Wright and Yeoman (1999a) presented data from this experiment which verified the HF Doppler technique, and hence the DOPE sounder, for the observation of small-scale particle-driven waves. The DOPE sounder and the CUTLASS Finland radar saw an identical frequency and amplitude wave simultaneously (figure 20). In addition, a large-scale resonant signature was detected by CUTLASS whilst the small-scale wave was occurring (Wright and Yeoman, 1999b). It was suggested that the large-scale size wave might have provided, through a non-linear Kelvin-Helmholtz instability, a seeding for the smaller scale wave, energy for the latter being provided by wave-particle interaction with drifting energetic ions. Bistatic CUTLASS radar velocity observations from this event were combined to produce electric field measurements with greater accuracy than any other instrument has been able to achieve to date. This is a result of the very narrow spectral widths associated with the artificial irregularities. These flow vectors were used to generate hodograms, indicating the amplitude and phase of the pulsation signatures; the first time that this has been done with HF radar data.

The group at the University of York ran the SP-UK-HUMS experiment during the October 1999 UK EISCAT campaign. This experiment attempted to use ULF period modulations with the Tromsø heater to modulate the local ionospheric conductivity above Tromsø. An attempt was made to modulate the existing ionospheric currents in the D-region and hence inject ULF Alfvén wave energy into the magnetosphere. This should result in the artificial generation of ULF pulsations. Since the Alfvén waves carry field aligned current, of which a significant proportion can be carried by precipitating particles in the auroral zone, a secondary objective was to investigate magnetosphere-ionosphere coupling. A particular aim was to experimentally test the predictions of magnetosphere-ionosphere feedback instabilities in using field-aligned currents to strongly couple magnetospheric and ionospheric dynamics. Data from EISCAT UHF, combined with magnetometer and optical instrumentation, were devoted to studying the artificially stimulated response.

12. EISCAT/CUTLASS studies

Over the first three years of operation of the CUTLASS Finland radar, from February 1995, the mainland EISCAT UHF system was run in CP-1 and CP-2 modes for a total duration exceeding 1000 hours. Simultaneous and spatially coincident returns from these two radars over this period provided the basis for a comparison of irregularity drift velocity and F-region ion velocity (Davies et al., 1999b). Initial comparison was limited to velocities from four intervals of simultaneous radar returns; intervals were selected such that they exhibited a variety of velocity signatures; subsequent comparison was made on a more statistical basis. The velocities measured by the two systems demonstrated reasonable correspondence over the velocity regime encountered during the simultaneous occurrence of coherent and incoherent scatter. Differences between the EISCAT UHF measurements of F region ion drift and the irregularity drift velocities from the Finland radar were explained in terms of a number of contributing factors. These included contamination of the irregularity drift velocities by E region echoes (a factor which was investigated further), and the potentially deleterious effect of discrepant volume and time sampling intervals.

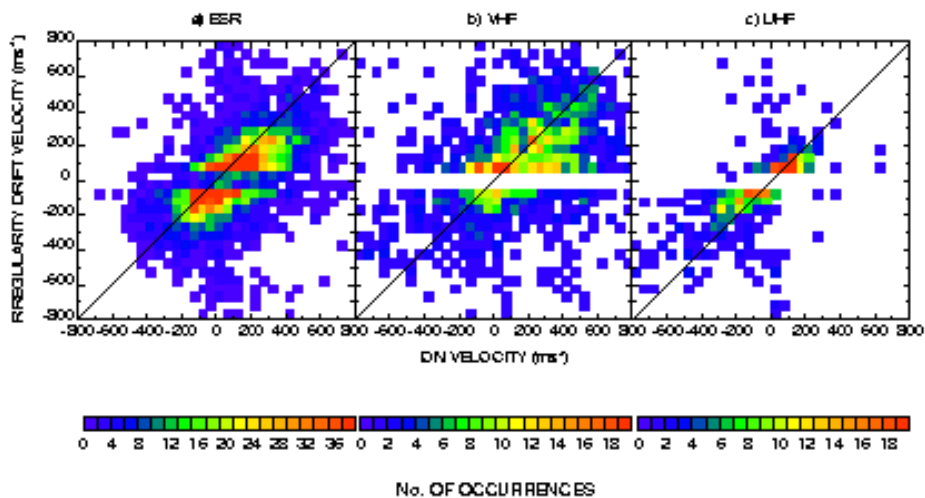


Figure 21 Scattergram of irregularity drift velocity measured by the Finland radar versus F-region ion velocity measured by the ESR (a) and along beam 1 of the VHF radar (b), during the SP-UK-CSUB experiments. Both ion velocity and irregularity drift speed are binned with a width of 50 m s^{-1} , with the number of observations in each bin represented by the colour scale to the right of the panel. Panel (c) reproduces the data from Davies et al. (1999b, in which ion velocity from the UHF radar is plotted against F-region irregularity drift velocity from the Finland radar. The solid lines indicate a hypothetical equality of irregularity drift and ion velocity.

During August 1998, SP-UK-CSUB, which combined operation of the mainland VHF and Svalbard UHF incoherent scatter radars, was run for several hours around magnetic midnight on four consecutive days. Davies et al. (2000) compared the bulk ion velocity measured by both the VHF and Svalbard radars during these experiments to irregularity drift velocity measurements by the CUTLASS Finland radar. The geometrical arrangement of the SP-UK-CSUB experiment – with both incoherent scatter radars directed at low elevation – offered a distinct advantage over the work of Davies et al. (1999b) as it enabled comparison over an extended range of latitudes. These latitudes, moreover, being poleward of those considered in the previous study where the nature of HF propagation somewhat limits coherent returns from the F-region. The agreement demonstrated by Davies et al. (2000), especially between the ion velocities measured by the EISCAT Svalbard radar and irregularity drift measurements by the Finland HF radar, was remarkable, as revealed in figure 21. This both confirms the belief that motion of irregularities in the F-region is governed by the plasma flow and, perhaps more importantly, does much to reassure the user of the scientific integrity of both data sets. The phase speed of irregularities generated artificially using the heating facility at Tromsø has also been compared to the bulk ion drift measurements from the EISCAT UHF system in a study reported by Eglitis et al. (1998b); this work indicated that such artificial irregularities drift also with the bulk plasma.

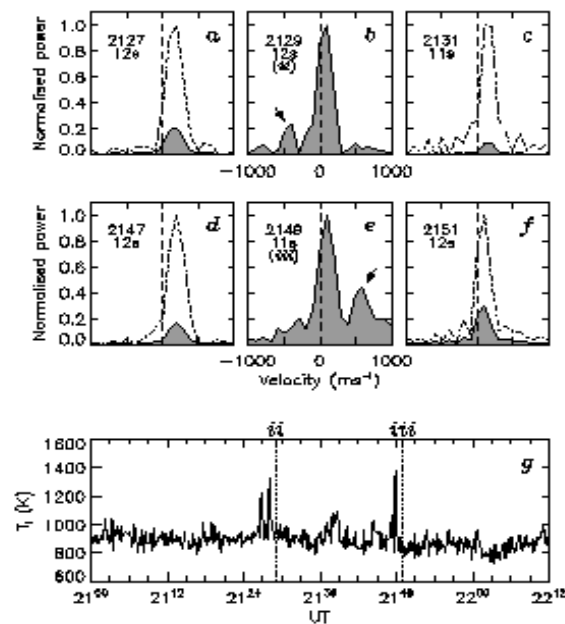


Figure 22 Six backscatter spectra observed by the CUTLASS Finland radar at the location of EISCAT (a to f). 10 s integration ion temperature as measured by EISCAT at an altitude of 301 km (g); the vertical dotted lines indicate the times of the CUTLASS soundings corresponding to panels b and e. A subsidiary peak appears in the CUTLASS spectra measured simultaneously with the ion temperature enhancements, an indication of high electric fields associated with auroral arcs.

Milan et al. (1999) presented a detailed examination of the characteristics of CUTLASS Finland HF radar backscatter interpreted with reference to the plasma parameters derived by the EISCAT UHF radar system, during a 12 hour interval from 18 and 19 June 1996. HF backscatter was found to exist only in regions of non-zero electric field, a factor necessary for the generation of F-region irregularities. Following a substorm expansion phase onset, the backscatter largely disappeared for a period of several hours, thought to be a consequence of non-deviative absorption of the HF radio wave in the D-region or a quenching of the F-region instability mechanism by enhanced E-region Pedersen conductivity. Moreover, the presence of auroral arcs within the coherent scatter volume identified from the EISCAT ion temperature observations, was found to increase the intensity of backscatter returns and introduces a subsidiary peak, displaced from the pre-existing peak, in the HF backscattered spectra. This subsidiary peak, results in an increase in the apparent spectral width of the backscatter (figure 22). This work, demonstrates clearly the complementary nature of HF coherent and incoherent scatter techniques, highlighting the substantive contribution to our understanding of the solar-terrestrial environment which can be made by use in concert of incoherent and HF coherent scatter radars.

Quasi-periodic fluctuations in the returned ground-scatter power from HF coherent scatter radars have been linked to the passage of medium-scale gravity waves. The location of the EISCAT mainland site, well within the CUTLASS HF Finland radar field-of-view, provided a unique opportunity for the gravity wave observing capabilities of the Finland radar to be assessed independently in work presented by Arnold et al. (1998). Results from 1 March 1995, when the EISCAT UHF radar was operating in its CP-1 mode, validated admirably the ability of HF radars to derive gravity wave information.

13. Magnetosphere-Ionosphere Coupling and Reconnection

A study of high-latitude coupling during an interval of changing IMF direction has been carried out at RAL in association with several other research groups in the UK and abroad (McCrea et al, 2000). Observations of the cusp and cleft ionosphere made by the ESR (figure 23) and Tromsø VHF radar on December 16 1998 have been compared with observations of dayside auroral luminosity made by Meridian Scanning Photometers at Ny Ålesund and HF radar backscatter observed by CUTLASS. The response of the cusp/cleft aurora was studied during a one-hour interval when the IMF turned from northward to southward, then back to northward again (figure 24). During the initial period of northward IMF, the aurora was situated poleward of the ESR. A strong equatorward expansion began when the IMF turned southward, and the ESR observed structured and elevated plasma densities and ion and electron temperatures. Cleft ion fountain upflows were seen in conjunction with the elevated ion temperatures and rapid eastward convection, consistent with the magnetic curvature force on newly-opened field lines for the observed negative B_y . Subsequently, the ESR remained poleward of the cusp/cleft aurora, and a series of poleward-moving events passed over it. After the last of these, the ESR was in the polar cap and the radar observations were characterised by very low densities and downward field-aligned flows. The IMF turned northward again, and the auroral oval contracted with the ESR moving back into the cusp/cleft aurora. In this poleward-retreating, northward-IMF cusp/cleft, convection flows were lower, upflows were weaker and the electron density and temperature enhancements were less structured. Following the northward turning, the bands of high electron temperature and cusp/cleft aurora bifurcated, suggesting that subsolar and lobe reconnection were taking place simultaneously.

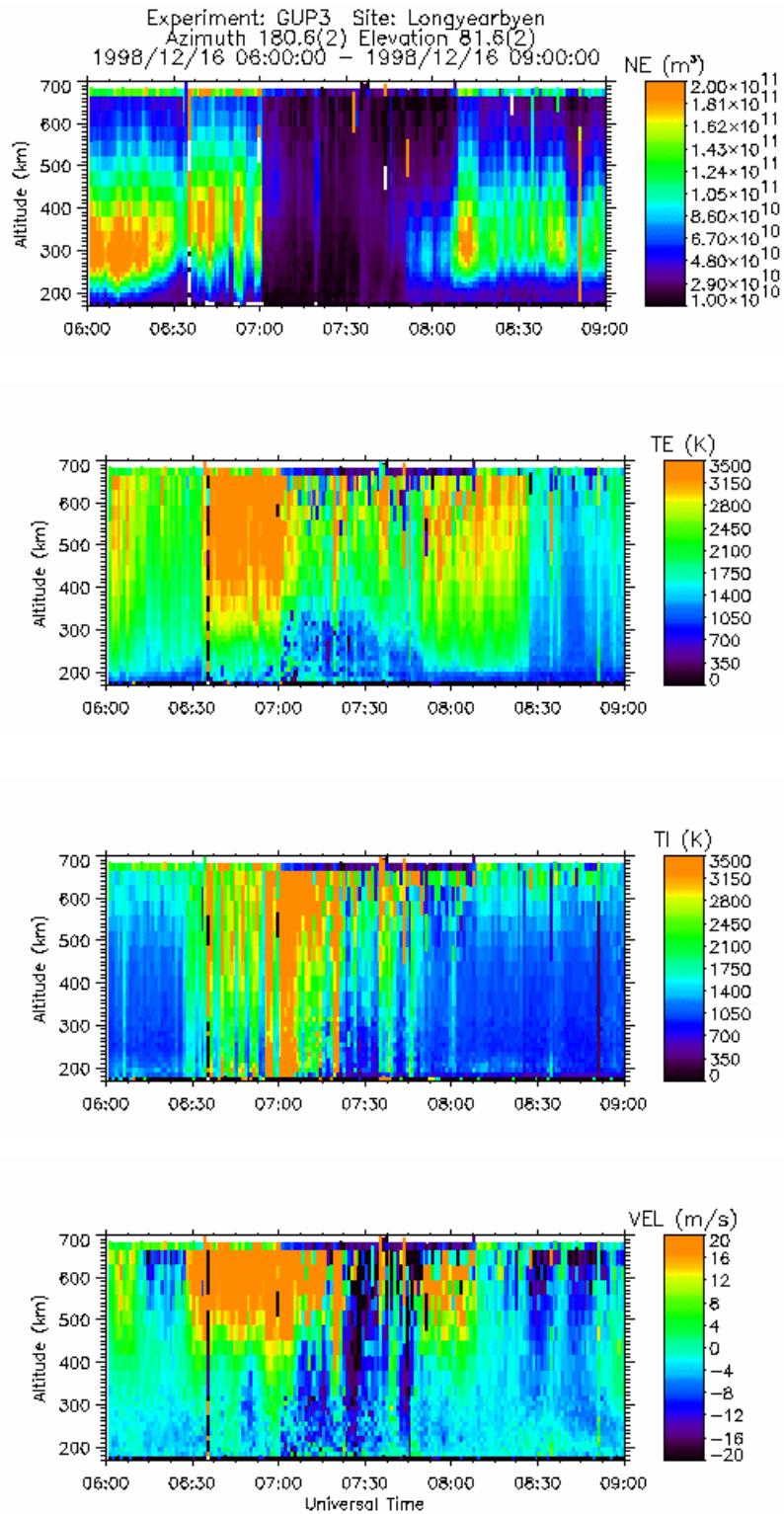


Figure 23 Multi-panel plot showing the variation of (from top to bottom) electron density, N_e , electron temperature, T_e , field-parallel ion temperature, T_i , and field-aligned velocity, V_{para} , with height and time, derived from the long pulse part of the ESR GUP3 experiment of the ESR on 16 December 1998.

More detailed studies of this interval have focussed on the behaviour of poleward-moving transients. Lockwood et al (2000) show that the behaviour of these events is similar to predictions for the modulating effect of pulsed reconnection. The rapid zonal flow, caused by the magnetic curvature force, is found to be a significant additional factor. In particular, the enhanced loss rates induced by the rapid convection can explain the way in which the 630 nm emission shows minima in brightness between poleward-moving events, which subsequently re-brighten as they move poleward. These observations are some of the first to show how poleward-moving transients appear in the ESR data, and represent a first step to identifying these features when supporting optical information is not available. A further discussion of how the observations of the poleward-moving transients compare to the behaviour expected from various models of their formation has been given by Thorolfsson et al (2000).

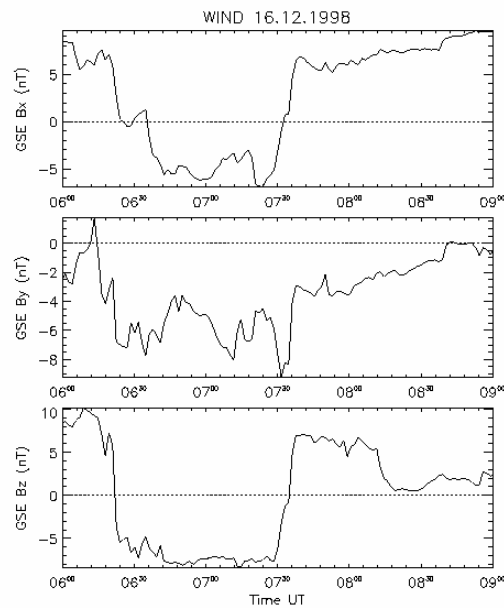


Figure 24 Plot showing the IMF components measured by the WIND spacecraft near Earth during the interval of ESR observations in figure 23

Interest in the coupling between the solar wind and the ionosphere provoked a major study involving observations by the EISCAT UHF radar, specifically a database of velocity measurements at 66.3° magnetic latitude from the CP-1 common programme (Khan, 1999; Khan and Cowley, 1999). The response time of these flows to changes in the north-south (Z) component of the IMF was investigated as a function of magnetic local time (MLT). This was done using a full cross-correlation analysis using the whole data set, and an event analysis keyed to sharp changes in the interplanetary magnetic field (IMF). Both techniques indicated that the response delays are shorter on the dayside than on the nightside, with average delays relative to first possible effects being around 3 minutes on the dayside, increasing to some 9 minutes on the nightside. Interpreted in terms of the propagation of flow effects from the dayside open-closed field line boundary, these values are consistent with an ionospheric expansion phase speed of the flow pattern of the order of 8 km s^{-1} . The results also indicated that the first effects usually appear in the post-noon sector, near 1400 MLT, an asymmetry which may relate to the typically spiral direction of the IMF.

Subsequent analysis, again based on the CP-1 velocity database, was performed to determine the influence of the Y-component of the IMF on ionospheric flows in the vicinity of EISCAT (Khan, 1999; Khan and Cowley, 2000). The effects were principally observed on the nightside, between dusk and early morning (~1600 to ~0200 MLT), where the east-west flow was found to depend upon IMF By with a gradient of between 20 and 40 m s⁻¹ per nT of By. Significant changes in flow are thus implied over the typical range of IMF By of ±5 nT. The flows were directed eastward for IMF By positive and westward for negative values of IMF By. The authors suggested that these changes in flow resulted from magnetic field distortions within the magnetosphere associated with a "penetrating" component of the interplanetary By. From this hypothesis, a fixed flow present in the equatorial plane of the magnetosphere will produce differing flows in the ionosphere due to the different mapping of the field lines. A theoretical model, set up on this basis, was found to produce flow changes, which agree quantitatively with the observed effect in terms of the flow direction, the sense of the effect, its amplitude, and the local time dependence.

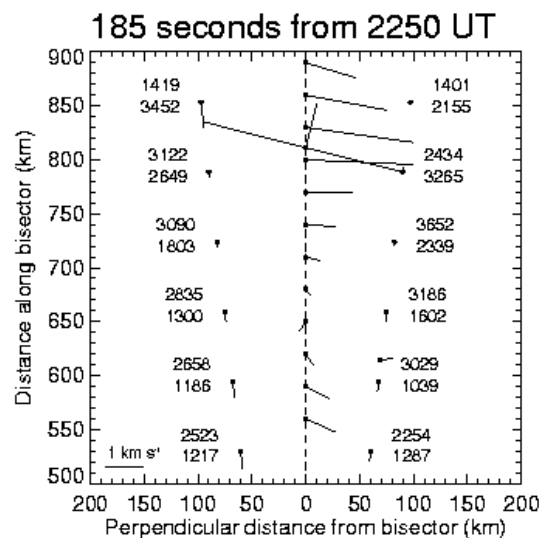


Figure 25 Plasma flow vectors in the VHF radar beam plane determined by combining line-of-sight velocities at points on the two beams which are equidistant from the instantaneous electron temperature boundary. Specifically, vectors have been derived at spatial points separated by 30 km along the bisector, using line-of-sight velocities suitably interpolated between range gates on the two beams according to the instantaneous orientation of the boundary during the 10 s measurement interval. The vectors are plotted on the bisector of the radar beams. The actual line-of-sight velocities measured are also plotted, using the same scale, at the centres of the range gates along the two beams, indicated by dots. The numbers associated with each gate give the electron temperature (upper) and ion temperature (lower), in K. The instantaneous orientation of the 2000 K electron temperature boundary is also shown, drawn as a straight line between the radar beams, together with its velocity at the bisector. The velocity shown is the three-dimensional velocity along the normal, projected onto the beam plane. The vector shown between gates 2 and 3 of beam 2 is a pseudo-flow vector determined from the horizontal magnetic perturbation at station BJO, assuming that the ground magnetic disturbance is wholly due to Hall currents in an ionosphere with a nominal conductivity of 10 Siemen. The vector has again been projected onto the beam plan, and has been drawn at a point that is connected along the local magnetic field with the point 110 km vertically above BJO. The panel shows results for the 10 s integration period centred at 185s after 2250 UT on 7 December 1992.

Analysis of flow data from EISCAT has, over the past decade, led to the development of a new paradigm of flow excitation and decay in the polar ionosphere. The basic elements of the picture are the time-dependent flows that are excited when pulses of flux transfer take place between open and closed field lines due to magnetic reconnection at the magnetopause and in the tail. These ideas have been reviewed by Cowley (1998), together with the data on which they were based. Flow excitation by reconnection at the dayside magnetopause, followed by flux transport to the tail, is now very well established. More recently, these ideas have been developed to provide detailed qualitative descriptions of how the dayside flows and cusp precipitation depend on the IMF, and how they reconfigure when the IMF changes. These ideas have been compared with cusp auroral and radar flow data, and have been found to provide an excellent basis of understanding (Sandholt et al., 1998). While dayside conditions thus seem to be reasonably well understood theoretically, the corresponding flow effects on the nightside which are expected to be associated with reconnection in the tail during substorms have proved more elusive (Cowley et al., 1998).

A multi-instrument study of one substorm interval, on 7 December 1992, revealed the occurrence of a surge of nightside polar cap flow into the substorm bulge after onset (Fox et al., 1999). A more detailed analysis of the split-beam EISCAT VHF radar data during this interval from the UK special programme SP-UK-CONV, was presented in a subsequent paper by Fox et al. (2000). The authors studied the ionospheric effects of the substorm bulge, which propagated polewards over Svalbard, having been initiated at lower latitudes some 10 minutes earlier. The bulge was associated with a poleward-propagating F-region electron temperature enhancement, which had a sharp poleward border, less than one radar gate (60 km) wide, which was taken to be due to soft electron precipitation. The propagation speed was determined to be around 1.5 km s^{-1} . An ion temperature enhancement of between 1000 and 2000 K was also found, straddling the electron temperature boundary, in a region $\sim 100\text{-}200 \text{ km}$ wide. The only reasonable explanation is in terms of a region of high plasma flow along the boundary, $1\text{-}2 \text{ km s}^{-1}$, and the consequent ion-neutral frictional heating. Careful analysis has shown the radar velocity data to be consistent with the presence of such flows, as shown in figure 25, which is taken to be produced by the strong change in ionospheric conductivity at the boundary, and the requirements of current continuity.

On August 21st 1998, a sharp southward turning of the IMF, following on from a 20 hour period of northward directed magnetic field, resulted in an isolated substorm over northern Scandinavia and Svalbard. At this time, EISCAT was running the UK special programme SP-UK-CSUB, which combined operation of both the mainland VHF and Svalbard UHF incoherent scatter radars. The former, in split beam mode, pointed northward at low elevation while the latter was directed southward, also at low elevation. The incoherent scatter observations have allowed the electrodynamics of the impulsive substorm electrojet, during its first few minutes of evolution at the expansion phase onset, to be studied in great detail (Yeoman et al., 2000). This was done with measurements from the CUTLASS HF coherent scatter radars, ground magnetometers and the Polar UVI imager. The expansion phase onset was characterised by a strong enhancement of the electron temperature and UV aurora. The initial flow response to the substorm expansion phase onset was a flow suppression within the substorm-disturbed electrojet, which extended up to some 300 km poleward of the initial region of auroral luminosity, imposed over a timescale of less than 10 s. The high conductivity region of the electrojet acts as an obstacle to the flow, resulting in low electric field in a region where the conductivity has not been enhanced. Rapid flows were observed at the edge of the high conductivity region. Subsequently the flow enhanced, flowing around the expanding auroral feature in a direction determined by the flow pattern prevailing before the substorm intensification. Lester (2000) has reviewed substorm phenomena, including their effects on EISCAT observations.

14. The Solar Wind

The programme of interplanetary scintillation measurements using EISCAT has continued, with significant progress being made in understanding the evolution of the inner solar wind. Earlier work had revealed that the solar minimum heliosphere was dominated by a clearly bimodal solar wind, with fast flow from coronal holes and slow flow above the streamer belt. When coronal holes extend towards the rotational equator of the Sun, interaction regions characterised by high densities and intermediate velocities at the leading edge, develop on the boundaries between fast and slow flow. During 1998 and 1999 several significant advances have been made in the programme of observations and in the analysis of data.

The main advance in the programme of observations has been the use of MERLIN to complement the EISCAT observations at 931 MHz with similar observations made at a far higher frequency thus extending the solar wind measurements closer to the Sun itself.

Over the last two years the group at the University of Wales, Aberystwyth, have also made significant improvements in analysis of the IPS data. The underlying principles remain the same – using coronal data to estimate the positions of regions of fast and slow flow across the ray-path and then using a 2-dimensional weak scattering model to determine the fast and slow flow speeds and relative densities. The fitting method has been improved and new methods of determining the position of fast and slow regions introduced:

- An improved method of fitting the IPS data has been adopted, in which the 2-D weak scattering model is used to fit the auto- and cross-spectra of the scintillations measured at the two sites rather than the calculated correlation functions (e.g. Breen et al., 1999). This method makes no assumptions about the shape of the correlation functions and so provides more accurate estimates of solar wind parameters. It also enables a correction to be included for the effects of wave propagation on the “scintillation velocity”, a more accurate estimate of bulk flow speed to be obtained. This correction is particularly important for observations close to the Sun, such as the MERLIN measurements made in May 1999.
- Beyond a heliocentric distance of about 10 R the fast solar wind expands at a near-constant velocity (Breen et al., 2000a) and very close to radially (Moran et al., 1998). Inside these limits the fast solar wind accelerates rapidly and expands equatorwards. The super-radial expansion of the fast wind means that a simple expansion model is not always accurate enough to associate features detected in IPS or in situ observations unambiguously with structures in the inner corona (inside 5-10 R). A more sophisticated model of coronal expansion is required so a numerical MHD model developed at Science Applications International Corporation, San Diego has been used to trace the solar wind back to its source regions. The Aberystwyth group has also used maps of coronal white-light intensity at 5, 10 and 20 solar radii generated from LASCO data to determine the location of coronal holes and thus regions of fast flow. By 20 solar radii the fast wind is expanding very close to radially and at effectively constant velocity, so maps from this distance provide a more accurate picture of the location of fast streams in the solar wind. The combination of LASCO data and MHD modelling has proved very successful in exploring structures in the low-activity solar wind (Breen et al., 1999) and is a great improvement over older methods when the Sun is more active (Breen et al., 2000c).

As a result of the developments the IPS technique made since 1997, the following scientific results have been established:

- Spaced-antenna measurements of interplanetary scintillation (IPS) are now internationally recognised as a powerful tool for probing the structure of the inner heliosphere, and EISCAT is recognised as a leading facility in solar wind research
- The results of the first Whole Sun Month (August 1996) showed that IPS observations are the ideal means of linking coronal and in-situ measurements

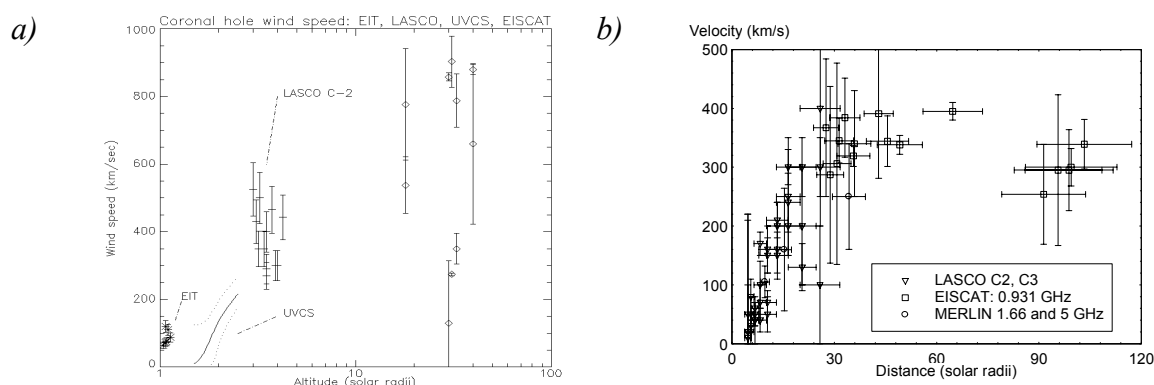


Figure 26 Velocity profiles for the fast (a) and slow (b) solar winds derived from simultaneous, co-ordinated observations from EISCAT, MERLIN and SOHO instruments (Breen et al., 2000a, Breen et al., 2000d)

- Simultaneous observations of solar wind streams with EISCAT, LASCO, UVCS, EIT, CDS and the SPARTAN 201-5 spacecraft have been carried out, confirming that the fast solar wind reaches 50% of its cruising speed inside 4 solar radii (September to October 1997, October to November 1998)
- Simultaneous observations of streams of slow solar wind using EISCAT, MERLIN and LASCO or less showed that the slow solar wind reaches its "cruising" velocity at heliocentric distances of 25 solar radii, with most acceleration taking place between 5 and 15 solar radii (May 1999).
- The early development of co-rotating interaction regions (CIRs) in the solar wind and their evolution with increasing distance from the Sun has been studied in detail and has shown that these structures exist at distances of 35 solar radii or less. This is consistent with the predictions of a simple model of the interaction region. The structure and development of fast stream/slow stream interfaces has been explored using EISCAT IPS data. EISCAT observations of the solar wind above coronal hole boundaries have allowed the velocity gradient between fast and slow winds to be estimated. The transition region appears to cover less than 5° in latitude, which is consistent with the results of radio occultation measurements and UVCS observations

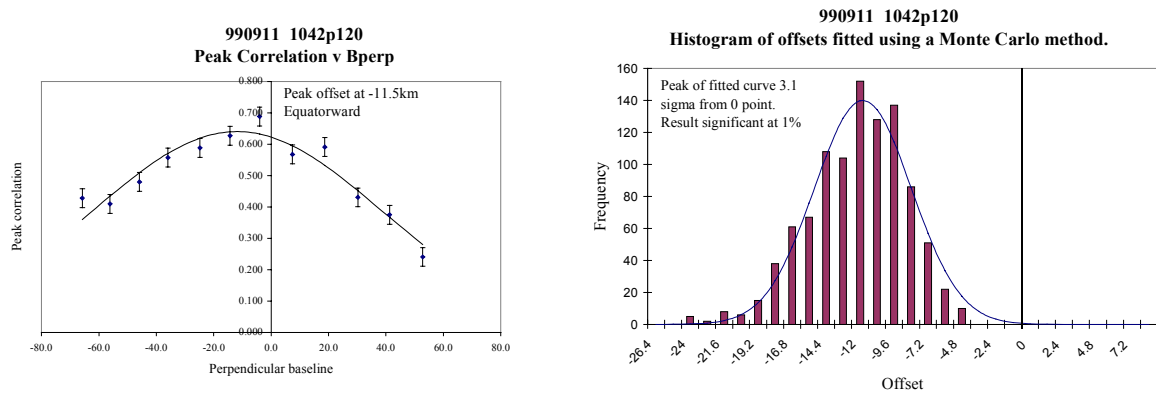


Figure 27 Off-radial flow in the fast solar wind, seen in an observation of 1042+120 on 11 September 1999 (analysed using the method described in Moran et al., 1998).

- The existence of an off-radial component of flow in the fast solar wind is now confirmed, and is consistent with the predictions of recent models of fast wind expansion. The results have been compared with Ulysses magnetic field measurements and there is good qualitative agreement between the two datasets. The super-radial expansion of the solar wind is always towards the heliomagnetic equator
- A preliminary study of the evolution of "halo" or geoeffective CMEs seen by both LASCO and EISCAT has been carried out. There is considerable evidence that CMEs approach the background solar wind velocity (by speeding up or by slowing down) between 20 and 70 solar radii
- EISCAT measurements have been used to study the evolution of the small-scale turbulent structure that gives rise to IPS. The scintillation power per unit path length is about twice as high in the slow wind as in the fast wind, with CMEs showing considerable enhancement above this level. These results are consistent with Nagoya, Ootacamund and Cambridge IPS measurements.

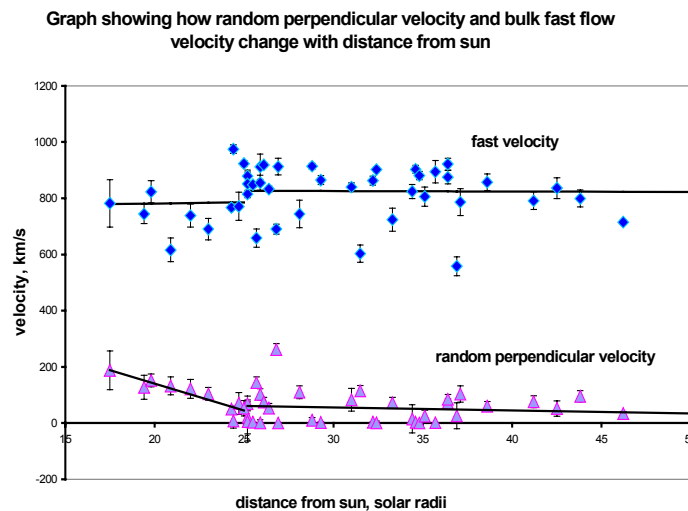


Figure 28 Bulk flow speed and random velocity perpendicular to the flow vector plotted as functions of heliocentric distance. Random perpendicular velocity is an indication of the amplitude of low-frequency Alfvén waves (presented at 1999 London MIST by Canals et al.)

- Detailed studies of turbulence in the fast solar wind have shown that the flux of low-frequency Alfvén waves increases at heliocentric distances inside 25 solar radii. This result has important implications for understanding the acceleration mechanism of the fast wind
- The evolution of the 3-D structure of the inner solar wind over the minimum and rising phase of the solar cycle has been studied. In conjunction with SOHO and Ulysses measurements, these results are leading to a significant improvement in our understanding of the evolution of the Sun as it approaches solar maximum.

15. Instrumentation and Techniques

Before installation on Svalbard, the new UCL-Southampton Imaging Spectrograph had its first test run during the solar eclipse on 11 August 1999. Results from the eclipse, for a 10-second exposure when the clouds parted are shown in figure 29. The emissions of hydrogen alpha, beta and gamma are all seen in this frame. In November 1999 the spectrograph and associated optical instruments were first used to measure auroral emissions during an EISCAT campaign in Ramfjordmoen. The first campaign to look for proton aurora was in December 1999 on Svalbard, using the ESR, when the dual barrel photometer and narrow angle imager were calibrated and installed to run under remote control. The assembly consists of a high-resolution, high sensitivity spectrograph (12 degree slit) mounted with two sensitive photometers (each 1 degree field of view) and a narrow-angle (12 by 8 degrees) sensitive video camera. Initial results were very encouraging. The narrow angle camera has proven so "popular" that the feed from the camera is to be used throughout the Adventdalen station, and a BAAS report on auroral morphology has been produced by an amateur astronomer using the facility. The photometers have been producing data regularly - as a remotely controlled observatory even after the campaign team left, measuring to a high sensitivity both nitrogen and hydrogen emissions. Some successful observations were carried out with the spectrograph itself, though detailed analysis is going to take some time.

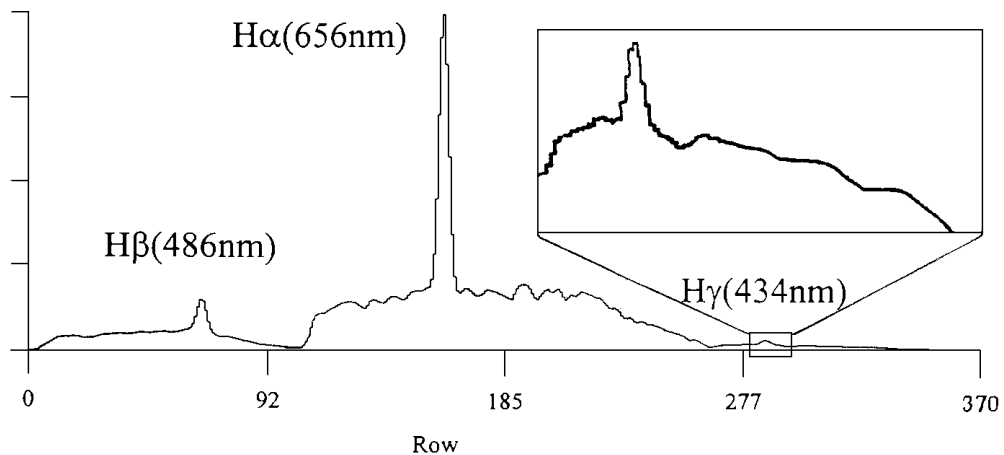


Figure 29 Composite spectrum of the Balmer α , β and γ lines acquired through clouds with the new imaging spectrograph during the total solar eclipse of 11 August 1999.

Appendix A: Papers produced by the UK EISCAT Community

1998

Arnold, N.F., T.B. Jones, T.R. Robinson, A.J. Stocker, and J.A. Davies, "Validation of CUTLASS HF radar gravity wave observing capability using EISCAT CP-1 data", *Ann. Geophysicae*, 16, 1392-1399, 1998

Balmforth H.F., R.J. Moffett and A.S. Rodger, "Modelling studies of the effects of cusp inputs on the polar ionosphere", *Adv. Space Res.*, 22, 1391-1394, 1998

Bernhardt, P.A., R.P. McCoy, K.F. Dymond, J.M. Picone, R.R. Meier, F. Kamalabadi, D.M. Cotton, S. Chakrabarti, T.A. Cook, J.S. Vickers, A.W. Stephan, L. Kersley, S.E. Pryse, I.K. Walker, C.N. Mitchell, P.R. Straus, H. Na, C. Biswas, G.S. Bust, G.R. Kronschnabl and T.D. Raymund, "Two dimensional mapping of the plasma density in the upper atmosphere with computerized ionospheric tomography (CIT)", *Physics of Plasmas*, 5, 2010-2021, 1998

Breen, A.R., P.J. Moran, C.A. Varley, W.P. Wilkinson, P.J.S. Williams, W.A. Coles, A. Lecinski and J. Markkanen, "Interplanetary scintillation observations of interaction regions in the solar wind", *Ann. Geophys.*, 16, pp.1265-1282, 1998

Cowley, S.W.H., "Excitation of flow in the Earth's magnetosphere-ionosphere system: observations by incoherent-scatter radar", in *Polar Cap Boundary Phenomena*, edited by A. Egeland, J. Moen, and M. Lockwood, Kluwer Academic Publ., Dordrecht, pp. 127-140, 1998

Cowley, S.W.H., H. Khan, and A. Stockton-Chalk, "Plasma flow in the coupled magnetosphere-ionosphere system and its relationship to the substorm cycle", in *Substorms-4*, edited by S. Kokobun and Y. Kamide, Terra Sci. Publ. Co., Tokyo, pp. 623-628, 1998

Davies J.A., M. Lester and I.W. McCrea, "Correction to "A statistical study of ion heating observed by EISCAT"" *Ann. Geophys.*, 12, 477-478, 1998

del Pozo C.F. and A.D. Aylward, "Ion line in the D and E-regions from EISCAT observations and the Lancaster-Sodankyla model", *Adv. Space Res.*, 21, 905-909, 1998

del Pozo C.F., E. Turunen and T. Ulich "Negative ions in the auroral mesosphere during a PCA event around sunset", *Ann. Geophys.*, 13, 782-793, 1998

Eglitis P. and T.R. Robinson, "Investigations of the phase speed and spectral width of high-latitude plasma irregularities", *Adv. Space Res.*, 21, 1361-1364, 1998

Eglitis P., I.W. McCrea, T.R. Robinson, T. Nygrén, K. Schlegel, T. Turunen and T.B. Jones, "New techniques for auroral irregularity studies with COSCAT", *Ann. Geophys.*, 12, 1241-1250, 1998a

Eglitis, P., T.R. Robinson, M.T. Rietveld, D.M. Wright, and G.E. Bond, "The phase speed of artificial irregularities observed by CUTLASS during HF modification of the auroral ionosphere", *Geophys. Res. Lett.*, 103, 2253-2259, 1998b

Frey H.U., S. Frey, B. S. Lanchester and M. Kosch, "Optical tomography of the aurora and EISCAT", *Ann Geophys.* 16, 1332-1342, 1998

Foster, C., M. Lester, and J.A. Davies, "A statistical study of diurnal, seasonal and solar cycle variations of F-region and topside auroral upflows by EISCAT between 1984 and 1996", *Ann. Geophysicae*, 16, 1144-1158, 1998

Jones G.O.L. and C.J. Davis, "Occurrence and characteristics of high-latitude mesospheric echoes at MF: observations by Halley and Tromsø dynasondes", *Journal of Atmospheric and Solar-Terrestrial Physics*, 60, 595-605, 1998

- Lanchester B. S., M.H., Rees, K.J.F. Sedgemore, J.R. Palmer, H.U. Frey and K.U. Kaila, "Ionospheric response to variable electric fields in small scale auroral structure", *Ann Geophys.* 16, 1343-1354, 1998
- Lühr H., A.D. Aylward, S.C. Buchert, A. Pajunpää, K. Pajunpää, T. Homes and S.M. Zalewski "Westward-moving dynamic substorm features observed with the IMAGE magnetometer network and other ground-based instruments", *Ann. Geophys.*, 12, 425-440, 1998
- Mitchell C.N., I.K. Walker, S.E. Pryse, L. Kersley, I.W. McCrea and T.B. Jones, "First complementary observations by ionospheric tomography, the EISCAT Svalbard Radar and the CUTLASS HF radar", *Ann. Geophysicae*, 16, 1519-1522, 1998
- Mitchell N.J. and V. St-C. Howells, "Vertical velocities associated with gravity waves measured in the mesosphere and lower thermosphere with the EISCAT VHF radar", *Ann. Geophys.*, 12, 1367-1379, 1998
- Moran, P.J., A.R. Breen, C.A. Varley, P.J.S. Williams, W.P. Wilkinson and J. Markkanen, "Measurements of the direction of the solar wind using interplanetary scintillation", *Ann. Geophys.*, 16, 1259-1264, 1998
- Pryse S.E., L. Kersley, C.N. Mitchell, P.S.J. Spencer and M.J. Williams, "A comparison of reconstruction techniques used in ionospheric tomography", *Radio Sci.*, 33, 1767-1779, 1998a
- Pryse S.E., L. Kersley and M.J. Williams "Electron density structures in the polar cap imaged by ionospheric tomography", *Adv. Space Res.*, 21, 1385-1390, 1998b
- Pryse S.E., L. Kersley, M.J. Williams and I.K. Walker, "The spatial structure of the dayside ionospheric trough", *Ann. Geophysicae*, 16, 1169-1179, 1998c
- Robinson, T.R., G.E. Bond, P. Eglitis, F. Honary, and M.T. Rietveld, "RF heating in a strong auroral electrojet", *Adv. Space Res.*, 21, (5)689-(5)692, 1998a
- Robinson, T.R., A. Stocker, G.E. Bond, P. Eglitis, D. Wright, and T.B. Jones, "First CUTLASS-EISCAT heating results", *Adv. Space Res.*, 21, (5)663-(5)666, 1998b
- Sandholt, P.E., J. Moen, P. Stauning, J.A. Holtet, S.W.H. Cowley, M. Lockwood, U.P. Løvhaug, T. Hansen, and A. Egeland, "Temporal and spatial variability of auroral forms in the 10-14 MLT sector: Relationship to plasma convection and solar wind-magnetosphere coupling", *Earth, Planets and Space*, 50, 663-682, 1998
- Schoendorf J. and W.L. Oliver, "A comparison of thermospheric oxygen density derived at EISCAT with values predicted by MSIS", *Geophys. Res. Lett.*, 25, 2119-2122, 1998
- Sedgemore K.J.F., J.W. Wright, P.J.S. Williams, G.O.L. Jones and M.T. Rietveld, "Plasma drift estimates from the dynasonde: comparison with EISCAT observations", *Annales Geophysicae*, 16, 1138-1143, 1998
- Spencer P.S.J., L. Kersley and S.E. Pryse, "A new solution to the problem of ionospheric tomography using quadratic programming", *Radio Sci.*, 33, 607-616, 1998
- Stocker A.J, "An overview of experimental observations made at Tromsø during heating at frequencies near harmonics of the electron gyrofrequency", *Adv. Space Res.*, 21, (5)653-(5)661, 1998
- Williams P.J.S., C.F. del Pozo and I.W. Hiscock, "Drift velocity of auroral arcs", *Adv. Space Res.*, 21, 1345-1348, 1998a
- Williams P.J.S., C.F. del Pozo, I.W. Hiscock and R. Fallows, "Velocity of auroral arcs drifting equatorward from the polar cap", *Ann. Geophys.*, 12, 1322-1331, 1998b
- Wright, D.M., T.K. Yeoman, and J.A. Davies, "A comparison of EISCAT and HF Doppler observations of a ULF wave", *Ann. Geophysicae*, 16, 1190-1199, 1998

1999

Balmforth H.F., R.J. Moffett and A.S. Rodger, "Localised structure in the cusp and high latitude ionosphere: a modelling study", *Annales Geophysicae*, 17, 455-462, 1999

Bogdanova, Y., V.S. Semenov, M.J. Buchan and R.P. Rijnbeek, "Auroral arc dynamics as a manifestation of magnetotail reconnection", in *Problems of Geospace 2*, edited by V. S. Semenov, H. K. Biernat, M. V. Kubyshkina, C. J. Farrugia and S. Mühlbacher, Austrian Academy of Sciences Press, pp.237-242, 1999

Breen, A.R., Z. Mikic, J.A. Linker, A.J. Lazarus, B.J. Thompson, P.J. Moran, C.A. Varley, P.J.S. Williams, D.A. Biesecker and A. Lecinski, "Interplanetary scintillation measurements of the solar wind during Whole Sun Month: linking coronal and in-situ observations", *J. Geophys. Res.*, 104, pp.9847-9870, 1999

Buchan, M.J., R.P. Rijnbeek, P.N. Smith, Y.V. Bogdanova, V.S. Semenov, I.W. McCrea, B. Holmeslet and J. Kultima, "Characteristics of poleward and equatorward moving auroral arcs in the nightside ionosphere", in *Problems of Geospace 2*, edited by V. S. Semenov, H. K. Biernat, M. V. Kubyshkina, C. J. Farrugia and S. Mühlbacher, Austrian Academy of Sciences Press, pp.243-248, 1999

Davies, J.A., and M. Lester, "The relationship between electric fields, conductances and currents in the high latitude ionosphere: A statistical study using EISCAT data", *Ann. Geophysicae*, 17, 43-52, 1999

Davies, J.A., M. Lester, and I.W. McCrea, "Solar cycle and seasonal dependence of ion frictional heating", *Ann. Geophysicae*, 17, 682-691, 1999a

Davies, J.A., M. Lester, S.E. Milan, and T.K. Yeoman, "A comparison of velocity measurements from the CUTLASS Finland radar and the EISCAT UHF system", *Ann. Geophysicae*, 17, 892-902, 1999b

Fox, N.J., S.W.H. Cowley, V.N. Davda, G. Enno, E. Friis-Christensen, R.A. Greenwald, M.R. Hairston, M.G. Kivelson, M. Lester, M. Lockwood, H. Lühr, D.K. Milling, J.S. Murphree, M. Pinnock, and G.D. Reeves, "A multipoint study of a substorm occurring on 7 December 1992 and its theoretical implications", *Ann. Geophysicae*, 17, 1396-1384, 1999

Khan, H., and S.W.H. Cowley, "Observations of the response time of high-latitude ionospheric convection and variations in the interplanetary field using EISCAT and IMP-8 data", *Ann. Geophysicae*, 17, 1306-1335, 1999

Honary F., T.R. Robinson, D. Wright, A.J. Stocker, M. Rietveld, and I.W. McCrea, "First direct observations of the reduced striations at pump frequencies close to the electron gyroharmonics", *Ann. Geophysicae*, 17, 1235-1238, 1999

Lockwood M. and S.W.H. Cowley, "Comment on "A statistical study of the ionospheric convection response to changing IMF conditions using the Assimilative Mapping of Ionospheric Electrodynamics technique" by A.J. Ridley et al", *J. Geophys. Res.*, 104, 4387-4391, 1999

Milan, S.E., J.A. Davies, and M. Lester, "Coherent HF radar backscatter characteristics associated with auroral forms identified by incoherent radar techniques: a comparison of CUTLASS and EISCAT observations", *J. Geophys. Res.*, 104, 22591-22604, 1999

Pudovkin, M.I., G.V. Starkov, P.N. Smith and R.P. Rijnbeek, "Dynamics of the dayside aurora and distribution of the electric fields during the breakup of auroral substorms", *Geomagnetism and Aeronomy* (in Russian), 1999

Sedgemore-Schulthess, K.J.F., M. Lockwood, T.S. Trondsen, B.S. Lanchester, M.H. Rees, D.A. Lorentzen, and J. Moen, "Coherent EISCAT Svalbard Radar spectra from the dayside cusp/cleft and their implications for transient field-aligned currents", *J. Geophys. Res.* 104, 24613, 1999

Semenov, V. S., Y. V. Bogdanova and R. P. Rijnbeek, "A new mechanism for interpreting the motion of auroral arcs in the nightside ionosphere", *Geophys. Res. Lett.*, 26, 2367-2370, 1999

Williams P.J.S., B. Jones, A.V. Kustov and M.V. Uspensky, "The relationship between E-region electron density and the power of coherent echoes at 45 MHz", *Radio Science*, 34, 449-458, 1999

Wright, D.M., and T.K. Yeoman, "CUTLASS observations of a high-m ULF wave and its consequences for the DOPE HF Doppler sounder", *Ann. Geophysicae*, 17, 1493-1497, 1999a

Wright, D.M., and T.K. Yeoman, "High resolution bistatic radar observations of ULF waves in artificially generated backscatter", *Geophys. Res. Lett.*, 26, 2825-2828, 1999b

Wright J.W. and M.V. Pitteway, "A new data acquisition concept for digital ionosondes: Phase-based echo recognition and real-time parameter estimation", *Radio Science*, 34, 871-882, 1999

2000

Bogdanova, Y., V.S. Semenov, R.P. Rijnbeek and P.N. Smith, "Analysis of auroral arc dynamics based on a model of magnetic reconnection in the magnetotail", *J. Atmos. Solar Terr. Phys.*, submitted, 2000

Boyd D.R.S., M. Sastry, I.W. McCrea, S.R. Crothers and C.J. Davis, "First application of virtual reality to EISCAT training and operations", *Ann. Geophys.*, submitted, 2000

Breen, A.R., C.F. de Forest, B.J. Thompson, J.F. McKenzie, A. Modigliani, P.J. Moran, C.A. Varley and P.J.S. Williams, "Comparisons of interplanetary scintillation and optical measurements of solar wind acceleration with model results", *Adv. Space Res.*, in press, 2000a

Breen, A.R., P.J. Moran, C.A. Varley, P.J.S. Williams, A. Lecinski, B.J. Thompson and L. Harra-Murnion, "Interplanetary scintillation measurements of the solar wind above low-latitude coronal holes", *Adv. Space Res.*, in press, 2000b

Breen, A.R., B. J. Thompson, M. Kojima, D.A. Biesecker, A. Canals, R.A. Fallows, J.A. Linker, A. J. Lazarus, Z. Mikic, P.J. Moran and P.J.S. Williams, "Measurements of the Solar Wind over a wide range of heliocentric distances - a comparison of results from the first three Whole Sun Months", *Journal of Atmospheric and Solar-Terrestrial Physics*, in press, 2000c

Breen, A.R., S.J. Tappin, C.A. Jordan, P. Thomasson, P.J. Moran, R.A. Fallows, A. Canals and P.J.S. Williams, "Simultaneous Interplanetary Scintillation and Optical Measurements of the acceleration of the Slow Solar Wind", *Annales Geophysicae*, submitted, 2000d

Bromage, B.J.I., D. Alexander, A.R. Breen, J.R. Clegg, G. Del Zanna, C.F. DeForest, D. Dobrzycka, N. Gopalswamy and B.J. Thompson, "Structure of a large low-latitude coronal hole", *Solar Physics*, in press, 2000

Davies, J.A., T.K. Yeoman, M. Lester, and S.E. Milan, "A comparison of F-region ion velocity observations from the EISCAT Svalbard and VHF radars with irregularity drift velocity measurements from the CUTLASS Finland HF radar", *Ann. Geophysicae*, in press, 2000

del Pozo C.F., F. Honary, S.R. Marple and E. Nielsen, "Study of Auroral Absorption During E-region Instability Conditions", *Annales Geophysicae*, submitted, 2000a

del Pozo C.F., F. Honary, N. Stamatou and M.J. Kosch, "Study of Substorm Activity from Combined IRIS, EISCAT and DASI Observations", *Journal of Atmospheric and Solar-Terrestrial Physics*, submitted, 2000b

del Pozo C.F., P.J.S. Williams, N.G.J. Gazey, K.J. Sedgemore, P.N. Smith, F. Honary and M. Kosch, "Multi-instrument Observations of the Dynamics of Auroral Arcs: A Case Study", *Annales Geophysicae*, submitted, 2000c

- Fox, N.J., S.W.H. Cowley, J.A. Davies, R.A. Greenwald, M. Lester, M. Lockwood and H. Lühr, "Ionospheric ion and electron heating at the poleward boundary of a poleward-expanding substorm-disturbed region", *J. Geophys. Res.*, submitted, 2000
- Jones G.O.L., C.J. Davis and R.E. Stockwell, "Dynasonde observations of electron concentration gradients above Tromsø", *Journal of Atmospheric and Solar-Terrestrial Physics*, submitted, 2000
- Khan, H., and S.W.H. Cowley, "Effect of the IMF By component in the overhead ionospheric flow at EISCAT: observation and theory", *Ann. Geophysicae*, submitted, 2000
- Lanchester B.S., D. Lummerzheim, A. Otto, M.H. Rees, K.J.F. Sedgemore-Schulthess, H. Zhu and I.W. McCrea, "Ohmic heating as evidence for strong field-aligned currents in filamentary aurora", *J. Geophys. Res.*, submitted, 2000
- Lester, M., "HF coherent scatter radar observations of ionospheric convection during magnetospheric substorms", *Adv. Polar Upper Atmos. Res.*, in press, 2000
- Lester, M., J.A. Davies, and T.K. Yeoman, "The ionospheric response during an interval of Pc5 ULF wave activity", *Ann. Geophysicae*, in press, 2000
- Leyser T.B., B.U.E. Brändström, B. Gustavsson, Å. Steen, F. Honary, M.T. Rietveld, T. Aso, and M. Ejiri, "Simultaneous measurements of high-frequency pump-enhanced airglow and ionospheric temperatures at auroral latitudes", *Advances of Polar Upper Atmosphere Research*, in press, 2000
- Lockwood M., I.W. McCrea, S.E. Milan, J. Moen, J.-C. Cerisier and A. Thorolfsson, "Plasma structure within poleward-moving cusp/cleft auroral transients: EISCAT Svalbard Radar observations and an explanation in terms of large local time extent of events", *Ann. Geophys.*, submitted, 2000
- McCrea I.W., M. Lockwood, J. Moen, F. Pitout, P. Eglitis, A.D. Aylward, J.-C. Cerisier, A. Thorolfsson and S.E. Milan, "ESR and EISCAT observations of the response of the cusp and polar cap to IMF orientation changes", *Ann. Geophys.*, submitted, 2000
- Moran, P.J., A.R. Breen, A. Canals, J. Markkanen, J. Padmanabhan, M. Tokumaru, P.J.S. Williams, "Observations of interplanetary scintillation during the 1998 whole sun month: a comparison between EISCAT, ORT and Nagoya data", *Annales Geophysicae*, submitted, 2000
- Pryse S.E., A.M. Smith, L. Kersley, I.K. Walker, C.N. Mitchell, J. Moen and R.W. Smith, "Multi-instrument probing of the polar ionosphere under steady northward IMF", *Ann. Geophysicae*, 18, 90-98, 2000
- Robinson T.R., R. Strangway, R.B. Horne, D.M. Wright, J.A. Davies, T.K. Yeoman, A.J. Stocker, M.T. Rietveld, C.W. Carlson and J.P. McFadden, "Spacecraft detection of magnetically guided waves artificially injected from the ionosphere into the magnetosphere and of the resulting stimulated electron precipitation", *Geophys. Res. Lett.*, submitted, 2000
- Rodger A.S., G.D. Wells, R.J. Moffett and G.J. Bailey, "The effects of time-varying electric fields on the ionosphere and thermosphere", *Annales Geophysicae*, submitted, 2000
- Safargaleev V., W. Lyatsky, N.G.J. Gazey, P.N. Smith and V. Krivolov, "The response of the azimuthal component of the ionospheric electric field to auroral arc brightening", *Ann. Geophys.*, 18, 65-73, 2000
- Sedgemore-Schulthess, K.J.F., and J-P. St.-Maurice, "Enhanced on-acoustic spectra and their interpretation", *Surveys in Geophysics*, submitted, 2000
- Sergienko T., B. Gustavsson, Å. Steen, U. Brändström, M. Rietveld, T.B. Leyser, and F. Honary, "Analysis of excitation of the 630.0 nm airglow during a heating experiment in Tromsø in February 16, 1999", *J. Physics and Chemistry of the Earth*, submitted, 2000

Thorolfsson A., J.-C. Cerisier, M. Lockwood, P.E. Sandholt, C. Senior and M. Lester, "Simultaneous optical and radar signatures of poleward-moving auroral forms", *Ann. Geophys.*, submitted, 2000

Yeoman, T.K., J.A. Davies, N.M Wade, G. Provan, and S.E. Milan, "Combined CUTLASS, EISCAT, and ESR observations of an isolated substorm", *Ann. Geophysicae*, submitted, 2000

Zhu H, A Otto, M H Rees, B S Lanchester and D Lummerzheim, "Ionosphere-Magnetosphere simulation of small scale structure and dynamics", *J. Geophys. Res.*, Submitted, 2000

PhD Theses

1998

Moran, P.J., "Interplanetary scintillation measurements of the solar wind using EISCAT", University of Wales

Wells, G.D., "Modelling studies of thermospheric heat inputs and cooling processes using a fully coupled global model of the Earth's upper atmosphere", University of Sheffield

1999

Buchan, M. "Optical and Radar Studies of the Nightside Auroral Ionosphere", DPhil thesis, University of Sussex

Khan, H., "Response of the high-latitude ionospheric convention to changes in the interplanetary medium", University of Leicester

Conference Proceedings

1998

Bogdanova, Y.V., V.S. Semenov, M.J. Buchan and R.P. Rijnbeek, "Characteristics of reconnection events in the magnetotail based on auroral arc motion in the ionosphere", in *Proceedings of the 21st Annual Meeting "Physics of Auroral Phenomena"*, Apatity, pp. 27-30, 1998

1999

Breen, A.R., D. Biesecker, R.A. Fallows, A. Lecinski, Z. Mikic, P.J. Moran and P.J.S. Williams, "Interplanetary scintillation observations of high-speed flow in the low-latitude solar wind", *Solar Wind 9 – Proceedings of the Ninth International Solar Wind Conference, Nantucket, Massachusetts, 1998*, pp. 317-320, AIP conference proceedings 471, 1999

Kosch M.J., F. Honary, N. Stamatiou, C.F. del Pozo and T. Hagfors. "The Morphology of Auroral Optical Emissions, Riometer Absorption and Energy of the Precipitating Particles", proceedings of the 25th Annual European Meeting (1998) on Atmospheric Studies by Optical Methods, Granada, Spain, 1999

Appendix B: UK EISCAT campaigns in 1998 and 1999

Campaign 56

Experiments From: 19 to 25 January 1998

Campaign Team:

Francis Sedgemore-Schulthess	Southampton	Svalbard	Campaign Manager
Steve Crothers	RAL	Svalbard	

<u>Hours Used:</u>	CAPE	6	
	CUSP	4	
	TOTAL	10	(10 hours ESR)

This was a UK contribution to an international campaign also involving Finland, Norway and Japan, in which a total of 46 hours ESR data were taken.

Campaign 57

Experiments From: 23 to 30 March 1998

Campaign Team:

Phil Williams	UWA	Tromsø / Svalbard	Campaign Manager
Vikki Howells	UWA	Tromsø	

<u>Hours Used:</u>	DUCT	8	
	TOTAL	8	(8 hours VHF)

The campaign team also assisted in the running of the CP2L and CP6B common programmes.

Campaign 58

Experiments From: 20 to 26 August 1998

Campaign Team:

Ian McCrea	RAL	Tromsø	Campaign Manager
Steve Crothers	RAL	Svalbard	
Steve Marple	Lancaster	Tromsø	
Johnny Rae	Leicester	Tromsø	
John Storey	Leicester	Tromsø	
Nigel Wade	Leicester	Svalbard	
Jim Wild	Leicester	Tromsø	

<u>Hours Used:</u>	TIDE	32	(16h mainland + 16 h ESR)
	OMOT	11	(6 h mainland + 5 h ESR)
	CSUB	32	(16h mainland + 16h ESR)
	TOTAL	75	(38 h mainland + 37 h ESR)

The TIDE experiment was run as a collaboration with Japan, which contributed 16 accounting hours (8 hours mainland time + 8 hours ESR time).

Campaign 59

Experiments From: 5 to 16 October 1998

Campaign Team:

Steve Crothers	RAL	Tromsø	Campaign Manager
Peter Chapman	Leicester	Tromsø	Technical Support
Jackie Davies	Leicester	Tromsø	
Steve Milan	Leicester	Tromsø	
Mick Parsons	Leicester	Tromsø	Technical Support
Gaby Provan	Leicester	Tromsø	
Matthew Wild	RAL	Tromsø	
Darren Wright	Leicester	Tromsø	

<u>Hours Used:</u>	HEAT	46.0	
	OUCH	15.0	
	TOTAL	61.0	(61 hours mainland time)

This campaign was run as a collaboration with Germany, which contributed an additional 12 hours of accounting time.

Campaign 61

Experiments From: 11 to 26 January 1999

Campaign Team:

Francis Sedgemore-Schulthess	Southampton	Svalbard	Campaign Manager
Vikki Howells	UWA	Tromsø	
Jim Wild	Leicester	Tromsø	

<u>Hours Used:</u>	CAPE	27	(11 h mainland, 16 h ESR)
	NOON	7	(7 h ESR)
	TOTAL	34	(18 h mainland, 16 h ESR)

This campaign was run in collaboration with Norway, Sweden and Japan, who contributed 24, 10 and 17 hours of accounting time respectively, as well as personnel to staff the radar sites.

Campaign 62

Experiments From: 12 to 18 February 1999

Campaign Team:

Steve Marple	Lancaster	Tromsø	Campaign Manager
--------------	-----------	--------	------------------

<u>Hours Used:</u>	SIDE	21	
	TOTAL	21	(21 h mainland)

This campaign was run in collaboration with Germany, which contributed 22 hours of accounting time.

Campaign 63

Experiments From: 2 to 17 May 1999

Campaign Team:

Ian McCrea	RAL	Tromsø	Campaign Manager
Owen Jones	BAS	Andøya / Tromsø	ALOMAR Support
Helen Middleton	UWA	Tromsø	
Dora Pancheva	UWA	Tromsø	

<u>Hours Used:</u>	DUCT	29	
	TOTAL	29	(29 hours mainland)

Campaign 64

Experiments From: 1 to 9 July 1999

Campaign Team:

Paul Gallop	RAL	Tromsø	Campaign Manager
Helen Middleton	UWA	Tromsø	

<u>Hours Used:</u>	TIDE	53	(27 h mainland + 26 h ESR)
	TOTAL	53	(27 h mainland + 26 h ESR)

This was a nine-day international campaign for the study of tides and planetary waves, run partly as a Common Programme and partly from contributions of Special Programme time from all of the EISCAT Associate countries.

Campaign 65

Experiments From: 16 to 30 October 1999

Campaign Team:

Alan Aylward	UCL	Tromsø / Svalbard	Campaign Manager (part 1)
Nigel Wade	Leicester	Tromsø	Campaign Manager (part 2)
Peter Chapman	Leicester	Tromsø	Technical Support
Ranvir Dhillon	Leicester	Tromsø	
Ian Furniss	UCL	Tromsø	Optical Support
Betty Lanchester	Southampton	Tromsø	
Ian McWhiter	UCL	Tromsø	Optical Support
Stu Robertson	Southampton	Tromsø	
Jim Wild	Leicester	Tromsø	
Darren Wright	Leicester	Tromsø	

<u>Hours Used:</u>	HEAT	18	
	HUMS	24	
	OUCH	30	
	ARCS	20	
	TOTAL	92	(92 hours mainland)

Campaign 66

Experiments From: 4 to 12 November 1999

<u>Hours Used:</u>	CASE	4	
	SIDE	2	
	TOTAL	6	(6 h mainland)

Nobody from the UK took part in this campaign. Staff from the other collaborating countries (Germany, Japan, Norway and Sweden) operated the radars. The campaign also included third-party time.

Campaign 67

Experiments From: 1 to 15 December 1999

Campaign Team:

Ian Furniss	UCL	SvalbardOptical Support
Ian McWhirter	UCL	SvalbardOptical Support
George Millward	UCL	Svalbard
Stu Robertson	Southampton	Svalbard

<u>Hours Used:</u>	NOON	9	
	CUSP	10	
	SPEC	24	
	ECUS	5	
	TOTAL	48	(48 h ESR)

This campaign was run in collaboration with Norway, which contributed 8 hours. The ESR ran on every day during this interval, and included 60 hours of Common Programme.

1999 Summary

In addition, a further 29 hours of IPSS time was used outside the periods of the campaigns listed above, between May and October 1999.

Although we have still not had an official figure from EISCAT, the estimated UK usage of EISCAT in 1999 was 326.5 hours (227 hours mainland, 106 hours ESR). This represents 99% of the mainland allocation and 88% of the ESR allocation. Note that the UK time allocations for 1999 were higher than normal, due to extra observing time purchased from France.

APPENDIX C: THE UK EISCAT USER COMMUNITY

University of Bath

	Telephone	User ID
Dr CN Mitchell	01225 826610	C.N.Mitchell

E-mail User ID @bath.ac.uk

Fax 01225 826305

Address

Department of Electronic and Electrical Engineering
University of Bath
Claverton Down
BATH BA2 7AY

British Antarctic Survey

	Telephone	User ID
Dr I.J. Coleman	01223 221586	I.J.Coleman
Dr.M.P. Freeman	01223 221543	M.P.Freeman
Dr R.M. Horne	01223 221542	R.Horne
Dr G.O.L. Jones	01223 221546	O.Jones
Dr M. Pinnock	01223 221534	M.Pinnock
Dr A.S. Rodger	01223 221551	A.Rodger

E-mail User ID @bas.ac.uk

Fax 01223 221226

Address

British Antarctic Survey
High Cross
Madingley Road
Cambridge CB3 0ET

Imperial College

	Telephone	User ID
Prof P. Cargill	0207 594 7773	p.cargill
Mr T.J. Stubbs	0207 594 7759	tj.stubbs

E-mail User ID @ic.ac.uk

Fax 0207 594 7772

Address

Space & Atmospheric Physics Group
The Blackett Laboratory,
Imperial College,
Prince Consort Road,
London SW7 2BW

Lancaster University

	Telephone	User ID
Dr. C.F. del Pozo	01524 594674	C.del.Pozo
Dr. J.K. Hargreaves	01524 593969	J.Hargreaves
Dr. F. Honary (STPNFC PI)	01524 593055	F.Honary
Mr. A.J. Kavanagh	01524 594674	A.J.Kavanagh
Mr. S. Marple	01524 592699	S.Marple
Mr. N. Stamatiou	01524 592699	N.Stamatiou
Mr. H. Tao	01524 592699	H.Tao

E-mail User ID @lancaster.ac.uk

Fax 01524-592713

Address

Ionosphere and Radio Propagation Group
Department of Communication Systems
Faculty of Applied Sciences
Lancaster University
Lancaster University LA1 4YR

Leicester University

	Telephone	User ID
Dr. N.F. Arnold	0116 2523548	nsa1
Mr. P.J. Chapman	0116 2523006/3560	pjc7
Prof. S.W.H. Cowley	0116 2231331	swhc1
Dr. J.A. Davies	0116 2523548	jaq
Mr. R.S. Dhillon	0116 2523565	rsd6
Prof. T.B. Jones (EISCAT Council Member) (Chair of STPNFC)	0116 2523561	tbj
Dr. H. Khan	0116 2523548	hk13
Dr. M. Lester (STPNFC PI)	0116 2523580	mle
Dr. S.E. Milan	0116 2523565	ets
Ms.G. Proven	0116 2522083	gp3
Mr. I.J. Rae	0116 2522083	ijr1
Prof. T.R. Robinson	0116 2523562	txr
Dr. A.J. Stocker	0116 2522520	sto
Mr. J. Storey	0116 2231302	js43
Mr. N.M. Wade	0116 2523568	nmw
Mr. J.A. Wild	0116 2522083	jaw11
Dr. D.M. Wright	0116 2523568	dmw7
Dr. T.K. Yeoman	0116 2523564	yxo

E-mail User ID@ion.le.ac.uk

Fax: 0116 2523555

Address

Radio & Space Plasma Physics Group
Department of Physics and Astronomy
University of Leicester
Leicester LE1 7RH

Rutherford Appleton Laboratory

	Telephone	User ID
Mr. S.R. Crothers	01235 446564	steve
Dr. C.J. Davis (STPNFC PI)	01235 446710	chris
Mr. I. Finch	01235 446535	ivan
Dr. K.S.C. Freeman	01235 446519	ken
Mr. P. Gallop	01235 445160	paul
Ms. V. St.-C. Howells	01235 445044	vikki
Prof. M. Lockwood (EISCAT Council Member) (STPNFC Member)	01235 446496	mike
Dr. I.W. McCrea (STPNFC PI) (EISCAT SAC Member)	01235 446513	ian
Miss E.L. Williams	01235 445759	liz

E-mail User ID@eiscat.ag.rl.ac.uk

Fax 01235 445848

Address

Rutherford Appleton Laboratory
Chilton
Didcot
Oxon OX11 0QX

University of Sheffield

	Telephone	User ID
Prof. G.J. Bailey	0114 2223744	G.Bailey
Mr. M.H. Denton	0114 2223708	M.Denton
Prof. R.J. Moffett	0114 2223780	R.Moffett
Dr. JM Rees	0114 2223782	J.Rees
Dr. Y.Z. Su	0114 2223793	Y.Su

E-mail User ID@sheffield.ac.uk

Fax 0114 2223739

Address

Upper Atmosphere Modelling Group
Applied Mathematics Department
Hicks Building
University of Sheffield
Sheffield S3 7RH

Sheffield Hallam University

	Telephone	User ID
Mrs. J. Porteous	0114 2253268	j.porteous
Dr. A.M. Samson	0114 2253305	a.m.samson
Ms. S. Woodall	0114 2254776	s.l.woodall

E-mail User ID@shu.ac.uk

Fax 0114 2253066

Address:

School of Science and Mathematics
Sheffield Hallam University
City Campus, Pond Street
Sheffield S1 1WB

Southampton University

	Telephone	User ID
Dr. B.S. Lanchester	023 8059 2049	bsl
Prof. M.H. Rees	023 8059 2048	mhr
Prof. H. Rishbeth	023 8059 2048	hr
Mr. S.C. Robertson	023 8059 2048	scr
Dr. K.J.F. Sedgemoor-Schulthess	023 8059 2048	kjs

E-mail User ID@phys.soton.ac.uk

Fax 023 8059 2048

Address

Upper Atmosphere Group
Department of Physics
University of Southampton
Southampton SO17 1BJ

University of Sussex

	Telephone	User ID
Mr. G.R. Lewis	01273 678662	G.R.Lewis
Dr. R.P. Rijnbeek	01273 678699	R.P.Rijnbeek
Dr. P.N. Smith	01273 678662	P.N.Smith

E-mail UserID@sussex.ac.uk

Fax 01273 678097

Address

Space Science Centre
Physics and Astronomy Subject Group
School of CPES
University of Sussex
Falmer
Brighton BN1 9QH

University College, London

	Telephone	User ID
Dr. A.L. Aruliah	0207 504 9017	anasuya
Dr. A.D. Aylward	0207 504 9021	alan
Dr. I. Furniss	0207 504 9026	ianf
Mr. E. Griffin	0207 504 9020	eoghan
Dr. I. Muller-Wodarg	0207 504 9019	ingo

Email User ID@apg.ph.ucl.ac.uk

Fax 0207 504 9024

Address

Atmospheric Physics Laboratory
Department of Physics and Astronomy
University College London
67-73 Riding House Street
London W1P 7PP

University of Wales, Aberystwyth

	Telephone	UserID
Dr. A.R. Breen	01970 622814	azb
Miss A Canals	01970 621907	aac99
Prof. L. Kersley	01970 622813	lek
Ms. H Middleton	01970 621902	hrm94
Dr. N.J. Mitchell (STPNFC Member)	01970 622802	njm
Dr. P.J. Moran	01970 622811	plm
Dr. D. Pancheva	01970 621902	ddp
Dr. S.E. Pryse	01970 622801	sep
Mr. A. Smith	01970 622821	ams93
Dr. T.S. Viridi	01970 622811	tsv
Dr. I.K. Walker	01970 622821	ixw
Prof. P.J.S. Williams	01970 622817	pjw

E-mail User ID@aber.ac.uk

Fax 01970 622826

Address

Department of Physics
University of Wales
Penglais
Aberystwyth
Dyfed SY23 3BZ

University of Warwick

	Telephone	User ID
Dr SC Chapman	01203 524916	S.C.Chapman

E-mail User ID@warwick.ac.uk.

Fax 01203 692016

Address

Space & Astrophysics Group
Physics Dept.
University of Warwick
Coventry CV4 7AL

York University

	Telephone	UserID
Dr. I.R. Mann (STPNFC PI)	01904 432240	ian
Dr. R.A. Mathie	01904 432279	rod

E-mail User ID@aurora.york.ac.uk

Fax 01904 432214

Address

Magnetospheric Physics Group
University of York
Heslington
York YO10 5DD